CHAPTER 7:
BICALUTAMIDE

CHAPTER-7: BICALUTAMIDE

7.1 Introduction:

Bicalutamide (BIC) is a non-steroidal anti-androgen used for monotherapy in treating prostate cancer(1). It causes dose dependent reduction in the Prostate specific antigen (PSA) levels. It has the potential of working wonders at all the stages of prostate cancer disease continuum(2). BIC binds to cytoplasmic androgenic receptors and competitively inhibits the androgenic action by producing distortion of the co-activator binding site, thereby stopping the initiation of gene transcription. It causes some central androgen blockade and not much affects the testosterone and LH levels. It is also approved for combination therapy along with LHRH analogue for treating metastatic prostate cancer. It possesses a longer $t_{1/2}$ and undergoes an extensive metabolism in liver(3).

Some of the major challenges currently faced by the current cancer treatment include the solubility and permeability limitations faced by most of the new chemical entities and anticancer agents. Another important challenge is reducing the side effects of the current chemotherapeutic treatment by aiming for tumour targeted therapy for cancer. The most recent advancement being “theranostics” in which simultaneous diagnosis and therapeutic treatment is possible by incorporating both the agents in a single carrier.

BIC comes under Biopharmaceutical classification system (BCS) Class II and suffers from solubility limitations, leading to dissolution and bioavailability issues. Thus, formulating a novel drug delivery system for this drug could open new avenues for increasing its effectiveness in prostate cancer treatment. To achieve this purpose a mesoporous silica nano delivery system was designed using MCM-41 carriers and thereafter functionalizing with ligands and surface moieties which help in achieving a targeted mesoporous system for the drug BIC.

The drug delivery systems were designed based on the pH stimuli based and another was based on targeting the receptors overexpressed in cancer like folate receptors. PAA polymer was used as a pH responsive material and coated onto the surface of MCM-41 MSNs via an aminated intermediate layer. This was based on the fact that environment of cancer cells is more acidic than that of the healthy cells. Also, certain receptors are found to be overexpressed in cancer cells like folate receptors. Folic acid was used as a ligand to target the overexpressed folate receptors in cancer.

Thus, in the present chapter the application of bare and functionalized MSNs as oral as well as intravenous targeted delivery agents for BIC in cancer therapy have been discussed in depth along with their biosafety aspects and efficacy.

The facile synthesis and functionalization strategy was adopted. Dissolution and Caco-2 Permeability study was performed and Pharmacokinetic data and biodistribution analysis was noted and cytotoxicity study was done on LNCaP and PC-3 prostate cancer cell lines. The cell death mechanism, cell killing efficiency and cellular uptake was determined. A thorough histological examination was done to adjudge their preliminary biosafety.

7.2 Materials and methods:

7.2.1 Chemicals and reagents

Pure anhydrous active pharmaceutical ingredient (API) Bicalutamide (BIC) was obtained as a sample gratis from Intas Pharmaceuticals Ltd, (Ahmedabad, Gujarat, India). Tadalafil (TAD) was kindly gifted by Ami life sciences ltd , Vadodara, Gujarat.

Chemicals required for preparation of dissolution media viz, hydrochloric acid, sodium acetate trihydrate, acetic acid, monobasic potassium phosphate, sodium chloride, sodium hydroxide, ammonium acetate and potassium dihydrogen phosphate were purchased from S.D. Fine Chem Ltd, Mumbai. Vital ingredients like pancreatin, pepsin, sodium taurocholate and Lecithin were

obtained from Sigma Aldrich, (St, Louis, USA). For diffusion study, dialysis tubes having cut-off Molecular weights (Mw) of 7000 g/mol and 3500 g/mol were purchased from Hi media laboratories, Mumbai.

Fluorescein isothiocyanate (FITC) and 4,6-Diamidino-2-Phenylindole Dihydrochloride (DAPI) staining dyes were purchased from SRL Chemicals (Mumbai).Analytical and HPLC grade reagents Methanol (MeOH) and AR grade DMSO, acetone and Dimethyl Formamide (DMF) were procured from Fischer Scientific, India. De-ionized water was used for the synthesis of NPs and throughout the entire work. All the chemicals were used without any further purification steps.

Human epithelial colorectal adenocarcinoma Caco-2 cells and Human prostate cancer cell lines PC-3 and LNCaP were procured from National Centre for Cell Sciences (NCCS), Pune (Maharashtra, India). Chemicals for cell culture and cytotoxicity study *viz;* Roswell Park Memorial Institute (RPMI) -1640 media, Dulbecco's modified eagle medium (DMEM), Antibiotic mixture containing penicillin and streptomycin solutions of concentration 1% and Fetal bovine serum (FBS) and other materials used in cell line study were purchased from HI media Laboratories (Mumbai, India). 3-(4, 5-dimethylthiazol-2-yl)-2, 5-diphenyltetrazolium bromide (MTT) were purchased from Sigma Aldrich (St Louis, MO, USA). The blood was collected from a healthy human volunteer from blood bank for carrying out haemolysis study. Molecular biology grade DMSO was purchased from SRL ltd. Annexin V-FITC apoptosis kit was obtained from BD Biosciences. Cell culture flasks, well plates and trans well inserts were purchased from HI media Laboratories. Lucifer yellow dye used in Caco-2 cell permeability study was procured from Thermo scientific India.

Four months old healthy male Swiss Albino mice (SAM) weighing 22-28g were provided by Zydus Research Centre, Ahmedabad, India for carrying out the pharmacokinetic and biodistribution studies. The experimental protocol was approved by the *Committee for the*

Purpose of Control and Supervision of Experiments on Animals (CPCSEA) and the Institutional Animal Ethics Committee (IAEC) having protocol number MSU/IAEC/2017-18/1724. Anticoagulant EDTA disodium salt was procured from Loba Chemie, Mumbai. All the animals were kept under standard laboratory conditions with free access to food and water and acclimatized to the animal facility for at least 7 days before starting the experimental procedures.

7.2.2 Synthesis of bare and functionalised MSNs

The synthesis of bare and surface functionalised MSNs were done as per the procedures described in chapter 5 section 5.2.

7.2.3 BIC loading

A novel immersion solvent rotary evaporator method was employed for BIC loading into MSNs. BIC was dissolved in methanol. This was followed by individual addition of MCM-41, MCM-41-A, PAA-MSN, FA-MSN to the flask in the drug: carrier mass ratio 1:1.5. The mixture was kept under continuous stirring for 2h. The solvent was evaporated at 70°C by rotary evaporator. The final products were labelled as BIC-MCM-41, BIC-MCM-41-A, BIC-PAA-MSN,BIC-FA-MSN. Loading and entrapment efficiency was determined by UV-VIS spectrometry at 272 nm wavelength for BIC using below equations.

$$Loading\ efficiency\ (\%) = \frac{Wt\ of\ drug\ BIC\ in\ MSNs\ (mg)}{Initial\ wt\ of\ BIC\ (mg)} \ldots (7.1)$$

$$Entrapment\ efficiency\ (\%) = \frac{Wt\ of\ drug\ BIC\ in\ MSNs\ (mg)}{Initial\ wt\ of\ BIC\ loaded\ MSNs\ (mg)} \ldots (7.2)$$

Complete loading of BIC into mesopores and its absence on external walls was confirmed by FT-IR, DSC thermograms and WXRD characterization.

7.2.4 Formulation development

As the commercial formulation of BIC is in tablet form, a tablet formulation is necessary. A tablet formulation was prepared for synthesised bare and amine decorated BIC nanoparticles

following a direct compression method. The BIC tablets were prepared combining different excipients as listed in following table 7.1. Single punch tablet machine equipped with punches of 9 mm diameter with flat faces was utilized and BIC-MSN tablets were punched. A detailed evaluation of prepared tablet was done for varied parameters as mentioned in IP. Furthermore, the compatibility study of drug with excipient was carried out which demonstrated lack of any interaction.

Sr No.	Excipient Name	Use	Amount
1	Sodium starch glycolate	Disintegrating agent	2-5%
2	Polyvinyl pyrrolidone	Binder	2-4%
3	Talc	Glidant	0.5-1%
4	Magnesium stearate	Lubricant, diluent	0.4-1%
5	Microcrystalline cellulose	Disintegrating agent in Direct compression	q.s.

Table 7.1. Composition of BIC-MSN tablets

7.2.5 In vitro study

7.2.5.1 In vitro dissolution study

Veego USP type II paddle apparatus was used to perform the dissolution study in 1000 mL dissolution media at 50 rpm maintaining 37 ± 0.5 ℃ temperature. The *in vitro* dissolution study was performed for BIC, Marketed Formulation (MF), BIC-MCM-41 and BIC-MCM-41-A in various media viz water (with addition of 0.5% SLS), FaSSGF, FeSSGF, FaSSIF, and FeSSIF (Fast and Fed state biorelevant media) to study the drug release pattern from non-functionalized and functionalized mesoporous systems in presence and absence of food. The composition of various dissolution media used is stated in Table 7.2. Samples were withdrawn at regular intervals and analysed by UV spectrophotometry at wavelength maxima of 272 nm. The data obtained was fitted to various kinetic models and best fit was determined.

Sr No.	COMPOSITION	Official media	FaSSGF	FeSSGF	FaSSIF	FeSSIF
1	Lecithin	-	20µM	-	0.75mM	3.75mM
2	Sodium taurocholate	-	80 µM	-	3mM	15mM
3	Pepsin	-	0.1g	-	-	-
4	Acetic acid	-	-	2.1g	-	8.65g
5	Sodium acetate	-	-	4.01g	-	
6	Sodium chloride	-	1g	13.85g	3.093 g	11.87g
7	Sodium Lauryl Sulphate	0.5%	0..5%	0..5%	0..5%	0..5%
8	Milk	-	-	500mL	-	-
9	Pancreatin	-	-	-	-	-
10	Monobasic potassium phosphate	-	-	-	1.977g	-
11	Sodium hydroxide	-	-	-	0.174 g	4.04g
12	pH	7.2	1.6	1.6	6.5	6.5
13	Deionized Water	Upto 1000 mL	Upto 1000 mL	Upto 1000 mL	Upto 500 mL	Upto 1000 mL

Table 7.2. Composition of various dissolution media used. (USP official MEDIA= Water (0.5%), Fast state simulated gastric fluid (FaSSGF), Fed state simulated gastric fluid (FeSSGF), Fast state simulated intestinal fluid (FaSSIF), Fed state simulated intestinal fluid (FeSSIF)).

7.2.5.2 Dissolution Kinetics study

The % cumulative release data obtained from dissolution study was fitted to various kinetic models and the best fit was determined based on the R^2 value, AIC criterion and Model selection criterion.

7.2.5.3 In vitro diffusion study

Phosphate buffer saline (PBS) media of different pH like 5.5, 6.8 and 7.4 was used to determine the in vitro release behaviour of BIC. A dialysis tube having cut-off Molecular weight (M_w) of 7000 g/mol was used to fill the suspension of BIC, BIC-MCM-41, BIC-MCM-41-A,BIC-PAA-MSNs and BIC-FA-MSN. Continuous magnetic stirring was provided and sink conditions were maintained properly by replacing withdrawn samples immediately with fresh PBS of respective pH. The withdrawn samples were analysed by measuring the fluorescence intensity by Spectrofluorometer keeping a fixed excitation wavelength of 260 nm and measuring

emission at 323 nm.

7.2.5.4 Diffusion kinetics study

To know the release mechanism governing BIC release, the release data was fitted into various kinetic models and the prime fit amongst them was adjudged based on the lowest AIC and highest Regression coefficient and (Model selection criteria) MSC values.

7.2.6 In vitro cytotoxicity study

7.2.6.1 Caco-2 cell line

Caco-2 cell line was procured from NCCS-Pune and maintained at 5% Carbon dioxide, 37℃ and complete RPMI-1640 with 20% FBS and 1% antibiotics (Pen-Strep solution). Lucifer yellow was used to check the membrane integrity.

For the purpose of studying cytotoxicity of BIC, BIC-MCM-41 and BIC-MCM-41-A MSNs. MTT assay was carried out on Caco-2 cells. Caco-2 cells were cultured at low passage number. The cells were maintained at 37℃ in an incubator and 5% Carbon dioxide supply in DMEM medium supplemented with 20%FBS and 1% Pen-strep solution to aid in avoiding any sort of contamination. The cells were seeded at a density of 10,000 cells per well in complete DMEM media in 96 well microtiter plates. This was followed by nanoparticle treatment for 24 and 72h n fresh incomplete DMEM medium in concentration range 0.1-100 µg/mL. Next, 100 µL MTT dye was added to each well and incubated for 4 h. Ultimately, 100 µL DMSO was added to solubilize the formazan formed. After elapsing of 10 min the plates were read at 590 nm using plate reader, % cell viability was calculated as per the formula given below.

$$\%Cell\ Viability = \frac{O.D._{sample} - O.D._{blank}}{O.D._{negative\ control} - O.D._{blank}} \times 100 \ldots\ldots\ldots (7.3)$$

Blank was devoid of any cells.

O.D. stands for optical density.

7.2.6.2 LNCaP and PC-3 cell lines

For the purpose of studying cytotoxicity of BIC, BIC-MCM-41 and BIC-MCM-41-A MSNs. MTT assay was carried out on Caco-2 cells. Caco-2 cells were cultured at low passage number. The cells were maintained at 37°C in an incubator and 5% Carbon dioxide supply in DMEM medium supplemented with 20%FBS and 1% Pen-strep solution to aid in avoiding any sort of contamination. The cells were seeded at a density of 10,000 cells per well in complete DMEM media in 96 well microtiter plates. This was followed by nanoparticle treatment for 24 and 72h n fresh incomplete DMEM medium in concentration range 0.1-100 µg/mL. Next, 100 µL MTT dye was added to each well and incubated for 4 h. Ultimately, 100 µL DMSO was added to solubilize the formazan formed. After elapsing of 10 min the plates were read at 590 nm using plate reader, % cell viability was calculated as per the formula given below.

$$\%Cell\ Viability = \frac{O.D._{.sample} - O.D._{.blank}}{O.D._{.negative\ control} - O.D._{.blank}} \times 100 \ldots\ldots\ldots (7.4)$$

Blank was devoid of any cells.

O.D. stands for optical density.

7.2.7 Caco-2 monolayer cell line permeability study:

The Caco-2 cells were grown on trans well inserts having 0.4µ pore diameter with 1.13 cm^2 area. The inserts were thoroughly washed with 25mM HBSS Hank's balanced salt solution and 7.4 pH. The integrity of the monolayer formed was tested by monitoring Lucifer yellow dye permeability across the layer. Time dependent transport of BIC loaded MSNs was studied in unidirectional apical to basal manner. The donor compartment (apical) was treated with 0.5 mL of transport solution i.e. HBSS containing 0.1 mg/mL BIC and basal side was treated with 1.5 mL of HBSS solution. The samples were analysed by HPLC equipped with fluorescence detector with excitation wavelength of 260 and emission measured at 323nm.

After incubation of 30, 60, 90, 120, 180, 240 and 300 min, 100µL aliquots were withdrawn from the receiver and replenished with same volume of fresh HBSS. The collected samples were further analysed by HPLC equipped with fluorescence detector. The apparent permeability coefficient (P_{app}) was measured using the following equation.

$$P_{app}=dQ/dt/A\times C_0*60\ldots(7.5)$$

Where,

P_{app}: Apparent permeability coefficient (cm/h)

dQ/dt: drug permeation rate (mg/min)

A: cross-sectional area *i.e.* 1.13 cm^2

C_0: Initial drug concentration in the donor compartment (mg/mL)

7.2.8 In vitro cellular uptake study

The results for MSN carriers and their qualitative and quantitative uptake by Prostate cancer cells have been discussed in section 6.3.6.

7.2.8.1 Intracellular qualitative uptake study by confocal microscopy

7.2.8.2 Intracellular quantitative uptake study by Flow cytometry

7.2.9 Evaluation of cell death mechanisms by apoptosis assay

Annexin V-FITC double stain apoptosis detection kit from BD Biosciences was used for determining percentage of apoptotic and necrotic cells by standard Fluorescence activated cells sorting (FACS) assay. LNCaP and PC-3 cells were seeded each at a density of 10^6 cells per well and incubated for 24 h. The cells were treated with BIC solution, BIC-MCM-41-A, BIC-PAA-MSN and BIC-FA-MSN and incubated for 24 h followed by cold PBS (4°C) wash. Untreated cells were taken as control. The washed cells were then stained using FITC-Annexin V apoptosis detection kit. Concisely, the cells were suspended in 1 mL of 1 × binding buffer at a concentration of 1 × 10^6 cells/mL. Further, 5µL of FITC-Annexin V and 5µL of PI were

added per 100µL of the suspension (1×10^5). After mild vertexing, the cells were incubated for 15 min in dark. Finally, 400 µL of 1 × binding buffer was added to each tube and analysed by FCM (4).

7.2.10 Haemolysis study

For the purpose of studying effect of NPs on RBCs blood was taken into the tubes containing Ethylene diamine tetra acetic acid (EDTA) solution. Microscopic images obtained were used to study extent of haemolysis qualitatively. Percentage haemolysis was quantified by UV-Vis spectroscopy. The plasma was removed from the blood by centrifugation at high rpm and obtained RBCs were washed with sterile isotonic PBS solution. The diluted RBC suspension mixed with isotonic PBS was taken as a negative control with no lysis being observed. Further, RBCs treated with surfactant Triton-X 100 were taken as a positive control for maximum lysis being exhibited here. A suspension in concentration range of 1-100 µg/mL of formulated NPs was taken for study. The positive control, negative control and RBCs with NPs suspension were incubated for 2 h. Post incubation images were taken on a microscope. Thereafter, centrifugation of samples was performed and supernatant was analysed UV-Vis spectroscopy at 580 nm. The percentage (%) haemolysis was calculated by the formula (6).

$$\%Hemolysis = \frac{A_{sample} - A_{Negative\ Control}}{A_{Positive\ Contol} - A_{negative\ Contol}} \times 100 \dots\dots\dots (7.6)$$

7.2.11 In vivo pharmacokinetic study

7.2.11.1 Pharmacokinetic study for oral formulation

The study protocol to evaluate the pharmacokinetic parameters upon administration to SAM mice was approved by Institutional animal ethics committee (IAEC) constituted as per the guidelines of Committee for the purpose of control and supervision on experiments on animals (CPCSEA), India. The protocol number was MSU/IAEC/2017-18/1724. About 4 months old

healthy SAM were obtained from Zydus research centre, Ahmedabad, Gujarat. All the mice were given free access to food and water and acclimatized to the animal care facility for at least 7 days before starting the experiment.

To study the oral bioavailability, mice were assigned into 5 groups including control. The other groups were administered oral dose equivalent to 10mg/kg BIC solution, BIC-MCM-41, BIC-MCM-41-A and MF by direct introduction into stomach using oral gavage.

About 0.3 mL of blood was collected from retro orbital vein of mice in EDTA containing centrifuge vials. The developed HPLC method consisted of ammonium formate (20mM) (pH 4) and ACN in the ratio 46:54 run on a waters symmetry 300 C-18 (250mm× 4.6mm×5µ) column with a flow rate of 1 mL/min detected on a fluorescence detector. Various Pharmacokinetic parameters were determined using an excel add-in.

7.2.11.1.1 Experimental:

7.2.11.1.2 Sample preparation:

Protein precipitation method was used in sample processing. Plasma was separated from the blood sample by centrifugation at 4000 rpm for10 min at 4℃. Processed sample was mixed with internal standard Tadalafil (TAD). Acetonitrile (ACN) was used as a precipitating agent. Supernatant was collected post centrifugation and quantified by HPLC equipped with a fluorescence detector.

7.2.11.1.3 Pharmacokinetic parameters evaluation

Various pharmacokinetic parameters viz; AUC, $t_{1/2}$, C_{max} and MRT were calculated using an excel add-in PK Solver from the data obtained.

7.2.11.2 Pharmacokinetic study for parenteral formulation

Four months old healthy male Swiss Albino mice (SAM) weighing 22-28g were obtained from Zydus research centre, Ahmedabad, Gujarat, India). All the animal experiments were performed in accordance with the protocols endorsed by the Institutional animal ethics

committee (IAEC) guidelines (protocol number MSU/IAEC/2017-18/1724). All the animals were kept under standard laboratory conditions and provided free access to food and water and acclimatized to the animal facility for suitable time.

For pharmacokinetic study mice were randomly divided into 5 groups and intravenously injected from the tail vein with a 0.5 CC U40 insulin syringe fitted with a 28-$g^{1/2}$ needle with 200µL of sterile suspension of free BIC (5 mg/kg) body weight, BIC-MCM-41-A, BIC-PAA-MSN,BIC-FA-MSN and control. The blood samples (0.3 ml) were collected at explicit time interims and stored in EDTA containing centrifuge vials. Further, plasma was separated by centrifugation at 4000 rpm for 10 minutes at 4℃. 100µL plasma was mixed with internal standard Tadalafil (TAD). The samples were precipitated by adding Acetonitrile (ACN) and again centrifuged at 10000 rpm for 10 min. The supernatants were collected and BIC was quantified using a HPLC equipped with a fluorescence detector. The parameters of HPLC method developed were ammonium formate (20mM) and ACN in the ratio 46:54 on a waters Symmetry 300 C-18 column (250mm× 4.6mm×5µ) at pH 4.0 with a flow rate of 1mL/min. Pharmacokinetic parameters viz C_{max}, T_{max} and AUC were calculated using an excel add-in.

7.2.11.3 In vivo biodistribution study and histological examination

For studying biodistribution of BIC and MSNs, in major organs, mice were assigned into 4 groups (n=3) including control, free BIC, BIC-MCM-41-A,BIC-PAA-MSN and BIC-FA-MSN. The experimental groups were administered sterile BIC suspensions and NP suspensions at dose of 5 mg/kg. Sterile saline injections (0.9% NaCl) at equivalent volumes were given to mice as control. Mice were sacrificed at 24 h after injection and major tissues like heart, liver, lung, kidney, brain and spleen were collected and weighed. Furthermore, PBS solution was added to each tissue sample by an equal volume to its weight and subjected to high speed homogenization. The mixtures obtained were centrifuged at 10000 rpm for 10 min. The supernatant was collected and extracted with methanol. The obtained solution was transferred

to centrifuge vials and subjected to evaporation. The dried residues were reconstituted in 100µL methanol. The amount of BIC in each tissue was quantified by HPLC equipped with a fluorescence detector with excitation at 260 and emission at 323 nm.

The major organs collected were fixed in 10 % formalin solution. The organs were embedded in paraffin and sectioned to 4um sections and placed onto the glass slides. The histological sections were stained with Haematoxylin and Eosin stain (H&E) and observed under microscope. This was performed to determine the *in vivo* toxicity of various BIC formulations.

7.2.12 Statistical analysis

The experiments were conducted thrice, and the results were expressed as the means and standard deviations from the triplicate experiments unless mentioned otherwise. The statistical analysis was performed by one-way ANOVA and p-values less than 0.05 were considered as significant.

7.2.13 Stability study of mesoporous silica nanoparticles

The stability study of synthesized MSNs i.e. BIC-MCM-41, BIC-MCM-41-A, BIC-PAA-MSN, and BIC-FA-MSN was performed as specified in ICH Q1A(R2). The synthesized nanoparticles were exposed to 40±2 ºC and 75±5 %RH conditions and sampling was done at 0^{th} day, 3^{rd} month and 6^{th} month and samples were analysed by DSC and LXRD.

7.3 Results and discussion

7.3.1 Solid state evaluation

7.3.1.1 Fourier Transform-Infra Red (FT-IR) spectroscopy studies

FT-IR spectra (Figure 7.1) provided proof of the manner in which successful synthesis and functionalization of MCM-41 mesoporous silica nanoparticles proceeded. The spectra of unfunctionalized MSNs was comparatively simple and major peaks could be easily assigned. In fig 7.1 a characteristic peak attributed to BIC could be seen. The cyanide and amide carbonyl groups were denoted by peaks obtained at 2227 cm^{-1}, 1685 $cm^{-1}$and 3341 cm^{-1}respectively.

Aromatic stretching due to phenyl group was observed at 708 and 833 cm^{-1}. Characteristic cyano and carbonyl group peaks were seen at wavenumbers 2230 and 1689 cm^{-1}respectively. In case of non-functionalized MCM-41 (b) & (c) asynthesised and calcinated MCM-41 could be distinguished by non-existence of C-H stretching (2954 and 2854 cm^{-1}) and deformation vibrations at 1452 cm^{-1}. In the spectra of calcinated MCM-41, stretching vibrations attributed to silanol groups gave a broad peak covering range of 3000-3750 cm^{-1}. Bands observed at 811 and 1085 cm^{-1} were dedicated to Si-O bond stretching. Successful grafting of amino groups onto MCM-41 NPs was confirmed by a characteristic peak of asymmetric N-H bending vibration obtained at 1590 cm^{-1}. This was further assisted by twinlets at 2930 and 2870 cm^{-1}. Newer absorption peaks appearing at 1551, 1650 and 1714 cm^{-1}credited to N-H bending, C=O stretching in amide group and carboxyl group respectively were indicative of successful decoration by PAA on MSNs. Weak band at 2832 cm^{-1} is attributed to vibrational C-H of CH_2 groups present in FA. Crest at 1511 cm^{-1} corresponds to aromatic ring vibrations of C=C of FA. The newer band at 1609 cm^{-1} is belongs to typical C=O vibration. The N-H stretching band at 3346 cm^{-1} is superposed to vibrational O-H band. The superposed bands at 1606-1539 cm^{-1} could be allocated to stretching C=N, bending N-H and O-H vibrations. Furthermore, complete encapsulation was also visible from the drug loaded mesoporous spectra of all MSNs.

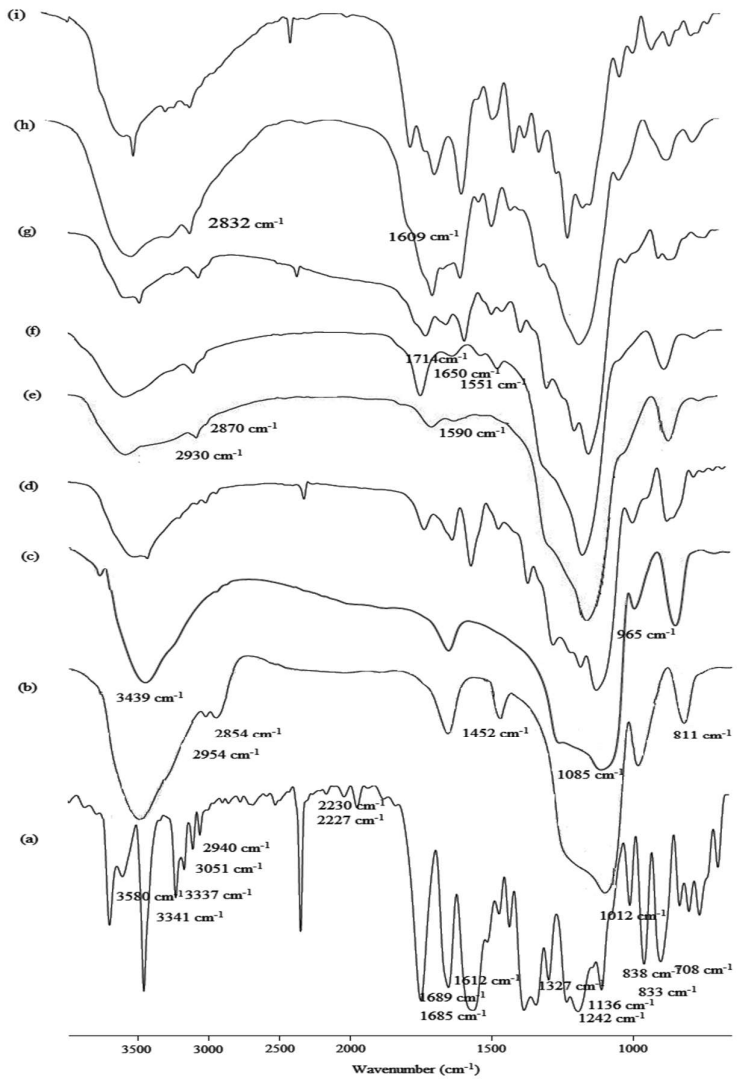

Figure 7.1. FT-IR Spectra (a) BIC (b) Asynthesised MSN (c) MCM-41 (d) BIC-MCM-41 (e) MCM-41-A (f) PAA-MSN (g) BIC-PAA-MSN (h)FA-MSN (i)BIC-FA-MSN

7.3.1.2 Differential scanning calorimetry (DSC) analysis

DSC was used in determining the melting point of the drug BIC and investigate complete entrapment at a preliminary level. The melting point of BIC was found to be 192.54 °C denoted by a sharp endothermic peak (Figure 7.2). The complete entrapment of drug into mesoporous carriers was confirmed by absence of any such peak in the thermogram.

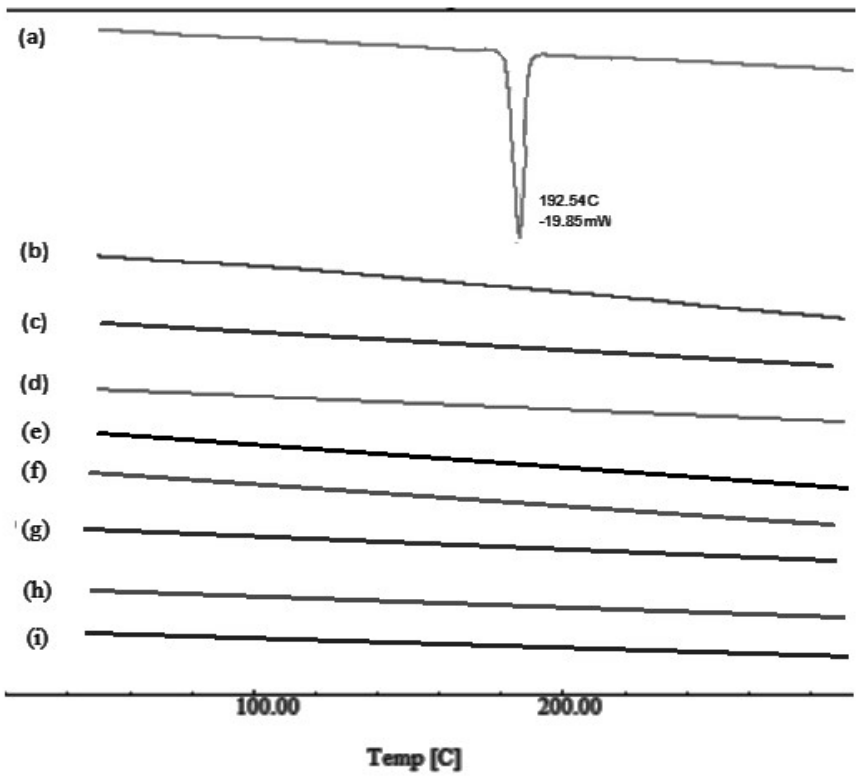

Figure 7.2. DSC thermograms of (a) Crystalline BIC (melting point of drug), (b) MCM-41 (c) BIC-MCM-41, (d) MCM-41-A (e)BIC-MCM-41-A (f) PAA-MSN (g) BIC-PAA-MSN (h) FA-MSN (i) BIC-FA-MSN

7.3.1.3 Thermogravimetric analysis

TGA analysis (Figure 7.3) was useful in determining the % of grafting moieties on MCM-41 along with the % drug loaded in both MCM-41 as well as MCM-41-A. Loss of surface silanol groups were the reason behind weight loss at higher temperature. Decomposition of various groups was evident in range 150-600℃. Although, a minor weight loss in the lower temperature reason could be credited to the surface dehydration by loss of water molecules. As calculated from the thermogram % grafting of amino groups was found to be 4.0%. The curves of surface functionalised PAA-MSN and FA-MSN exhibited a decreased weight loss attributed to silanol group reduction post functionalization.

The % of BIC loaded into MCM-41 was MCM-41-A was 38.95 and 36.15 % respectively as estimated by TGA. UV estimation gave a % loading of 39.12 and 37.19 respectively for MCM-41 and MCM-41-A.

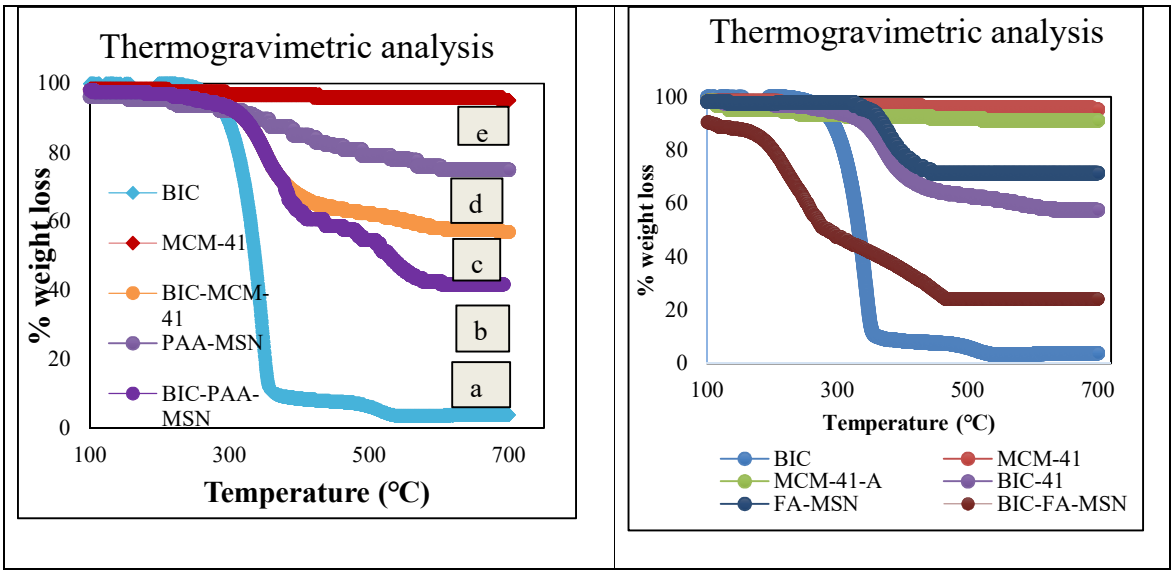

Figure 7.3. TGA of different nanocarriers and formulations BIC,MCM-41-A, BIC-MCM-41-A, BIC-PAA-MSN, PAA-MSN, BIC-MCM-41,MCM-41, FA-MSN and BIC-FA-MSN

7.3.1.4 Wide angle X-Ray diffraction analysis (W-XRD)

Crystalline nature of BIC was justified by the sharp and highly intensified peaks obtained in the wide angle XRD spectra (Figure 7.4). The position of the peaks identified in order of their ascending theta values are 12.29, 18.15, 23.29, 24.11, 29.1, 29.30, 31.45, and 34.82Θ. When we see the Wide-angle spectra of drug loaded MSNs, no clear intense peak is visible. This indicates the conversion of crystalline BIC to amorphous form after entrapment into MSNs. This fact could play a major part in dissolution enhancement of drug. The spectra of drug loaded bare and functionalised MSNs indicated a complete entrapment of drug into the mesopores.

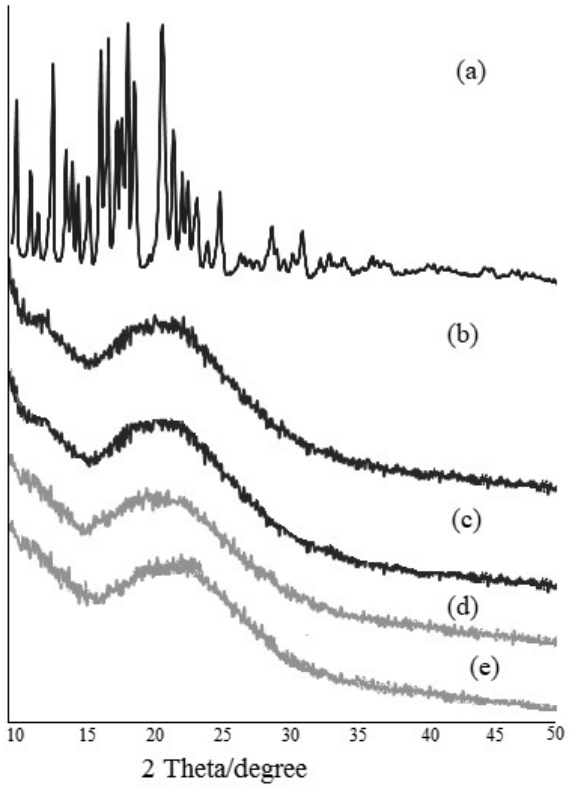

Figure 7.4. WAXRD spectra (a) BIC (b) BIC-MCM-41 (c) BIC-MCM-41-A (d) BIC-PAA-MSN (e) BIC-FA-MSN

7.3.1.5 Low angle X-Ray diffraction

Small angle and wide-angle X-Ray diffraction studies were carried out to ensure the integrity of mesoporous skeleton as well preserved and transition of nature of drug. In small angle XRD spectra three peaks characteristic to MCM-41 mesoporous carriers were obtained at 100, 110 and 200 reflection peaks (5). The characteristic peaks in MCM-41 were clearly visible. This pattern was well preserved and even after functionalization and drug loading as seen from the figure 7.5.

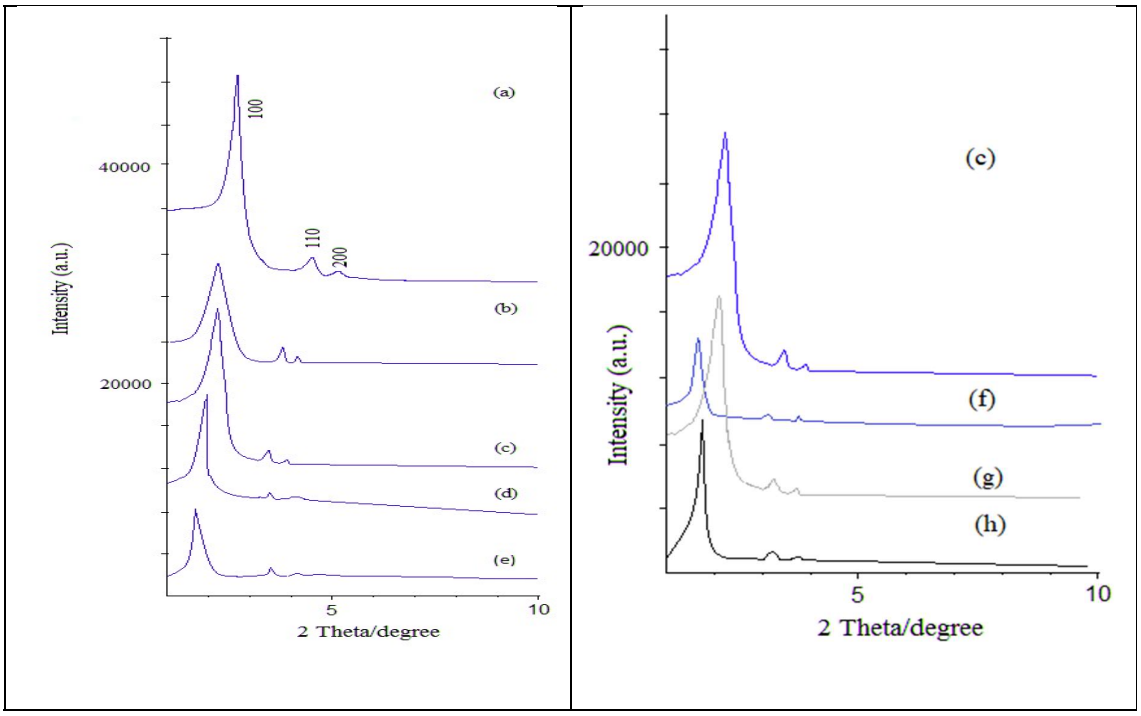

Figure 7.5. (a) LXRD Patterns of (a) MCM-41 (b) BIC-MCM-41 (c) MCM-41-A (d) PAA-MSN and (e) BIC-PAA-MSN (f) BIC-MCM-41-A (g) FA-MSN (h) BIC-FA-MSN

7.3.1.6 Zeta potential and size determination:

The zeta potential values changed as the surface coating proceeded further and post drug loading indicating the successful completion. Further, the size or the hydrodynamic diameter increased as the coating proceeded further(table 7.3).

Sr no	SAMPLE	HYDRODYNAMIC SIZE	ZETA POTENTIAL
1	MCM-41	110.2	-36.86
2	BIC-MCM-41	-	-24.74
3	MCM-41-A	124.7	+33.92
4	BIC-MCM-41-A	-	+36.98
5	PAA-MSN	142.85	-31.15
6	BIC-PAA-MSN	-	-20.86
7	FA-MSN	135.38	+36.04
8	BIC-FA-MSN	-	+28.56

Table 7.3. Zeta potential and size data for bare, surface functionalized and drug loaded MSNs

7.3.1.7 Nitrogen sorption analysis:

The adsorption-desorption isotherms obtained were having well defined capillary condensation step exhibiting type 4 characteristics (figure 7.6). This was evident of mesopores being homogenous in size (6). Highest surface area and pore size was observed for MCM-41 mesoporous carrier. Amine functionalized mesoporous carrier displayed decrease in the porosity and surface area as compared to their bare counterparts. Similarly, both the properties also decreased when drug was loaded into the mesopores due to the pores being occupied by drug molecules. The results are summarized in Table 7.4. Since the wall of the pores are covered by surface moieties the surface area and porosity was found to decrease as the functionalisation proceeded further.

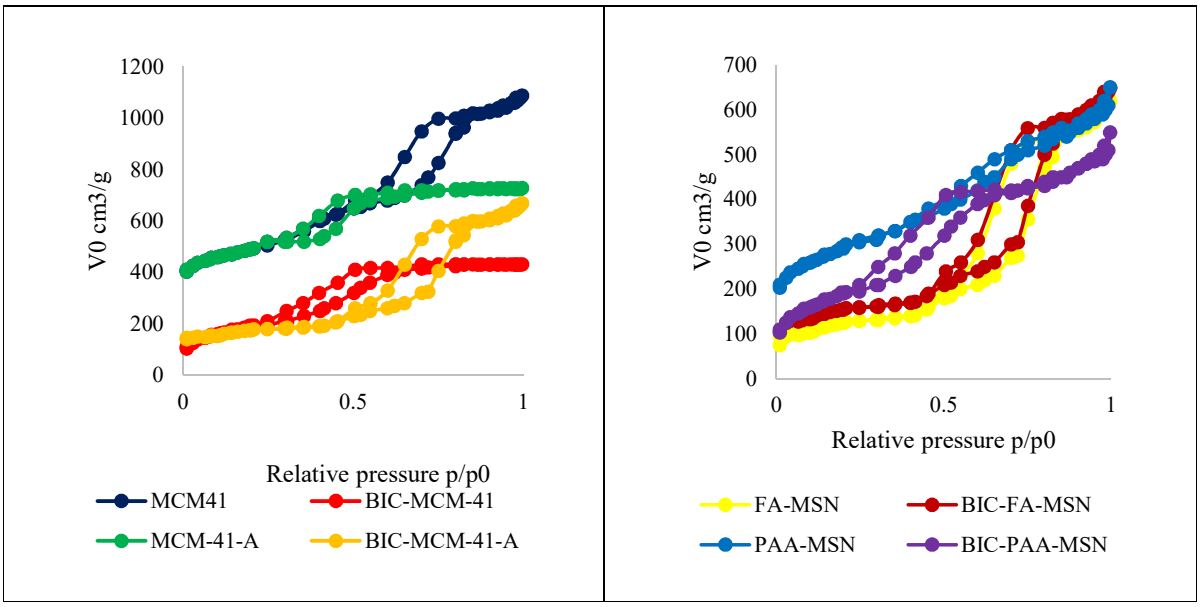

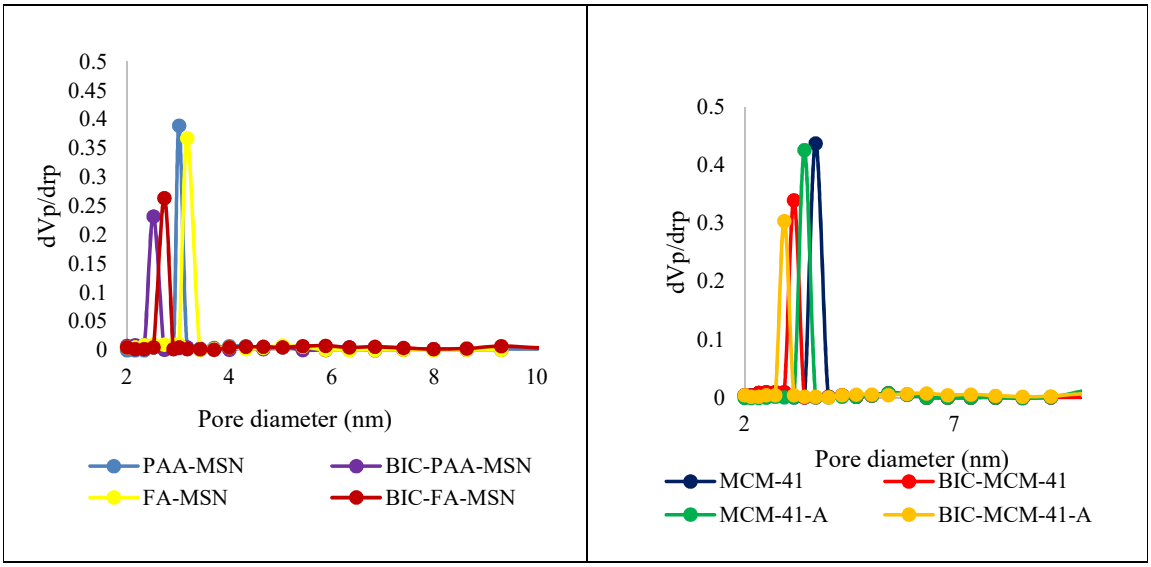

Figure 7.6. Surface area and porosity details of bare and BIC loaded formulations

Sr No	Parameters	MCM-41	MCM-41-A	BIC-MCM-41	BIC-MCM-41-A	PAA-MSN	BIC-PAA-MSN	FA-MSN	BIC-FA-MSN
1	BET Surface (m^2/g)	1089.97	827.90	813.28	762.12	702.84	501.38	745.72	530.25
2	BJH (surface area (m^2/g)	1441.97	1165.49	902.26	798.04	878.34	619.23	921.87	670.66
3	Pore size (nm)	3.69	3.43	3.13	2.91	3.02	2.61	3.22	2.83
4	Pore volume (cm^3/g)	0.4377	0.4261	0.3397	0.3041	0.3895	0.2319	0.3672	0.2639

Table 7.4. Porosity and surface properties of MSNs

7.3.2 Estimation of drug loading efficiency

The pore size and pore volume also contribute in determining the maximum amount of drug which can be entrapped in MSNs. A slight reduction in loading percentage from MCM-41 to post functionalization in MCM-41-A was observed.

Additionally, the TGA data also prove the thermal stability of silica materials for proposed potential application as site directing carrier for BIC. The TGA data exhibited extent of grafting as 4% in case of MCM-41-A,20.19% in PAA-MSNs and 23.75% in case of FA-MSNs

respectively. The % loading and entrapment estimated by UV spectrophotometry is summarized in Table 7.5. A healthy loading and entrapment percentage was obtained for all the mesoporous carriers.

Sr No.	Sample	DRUG: MSN Ratio	Percentage Loading		Percentage Entrapment
			By TGA	By UV	
1	BIC-MCM-41	1:1.5	38.95	39.12	96.48
2	BIC-MCM-41-A	1:1.5	36.15	37.19	91.72
3	BIC-PAA-MSN	1:1.5	33.28	39.12	82.00
4	BIC-FA-MSN	1:1.5	35.02	35.68	87.99

Table 7.5. Drug loading and % grafting of functional groups.

7.3.3 In vitro release study:

7.3.3.1 In vitro dissolution study

Drug release study was carried out in 1000 mL water with 0.5% SLS to determine the release pattern by calculating the cumulative drug release at different time points. BIC release from MCM-41 was highest followed by marketed formulation. However, a controlled and sustained behaviour of drug release was obtained in case of amine functionalized MSNs. Additionally, fast and fed state gastric and intestinal media were used to study if there is any effect of food on drug release from all the formulations (7). The drug release was almost similar in case of both fast and fed state conditions and hence it could be concluded that presence of food did not alter drug release (Fig 7.7). Thus, the medication could be taken either ways empty or after meal, it wouldn't affect the absorption or release. Further, various dissolution kinetic models were applied on the obtained %CDR data. Of the various models applied he highest regression coefficient and MSC value along with lowest AIC criteria was best fit in Weibull model in case of MCM-41 type mesoporous matrix (8) (Table 7.6 and 7.7). Whereas, in case of MCM-41-A matrix Higuchi model was found to the best fit satisfying all the three criteria (Table 7.7). Best fit models were understandably different for both release systems as a different release pattern was seen in both. MCM-41 gave an initial burst release and faster one as compared to somewhat

slower and sustained release action as observed in aminated matrix.

In vitro drug dissolution studies and kinetic modelling gave some useful results. A characteristic burst release pattern was observed in case of drug loaded MCM-41 NPs. Comparatively, a slow release was seen in amine functionalized mesoporous nanoparticles. Thus, the best fit models were also different in both the cases. In case of MCM-41, Weibull model was found to be the best fit one. Also, for MCM-41-A Higuchi model was the best fit one. Linear relationship between the fraction of release of BIC and square root of time, suggested a Higuchi diffusion process. This was again complementary to the AIC and MSC values obtained for Higuchi model.

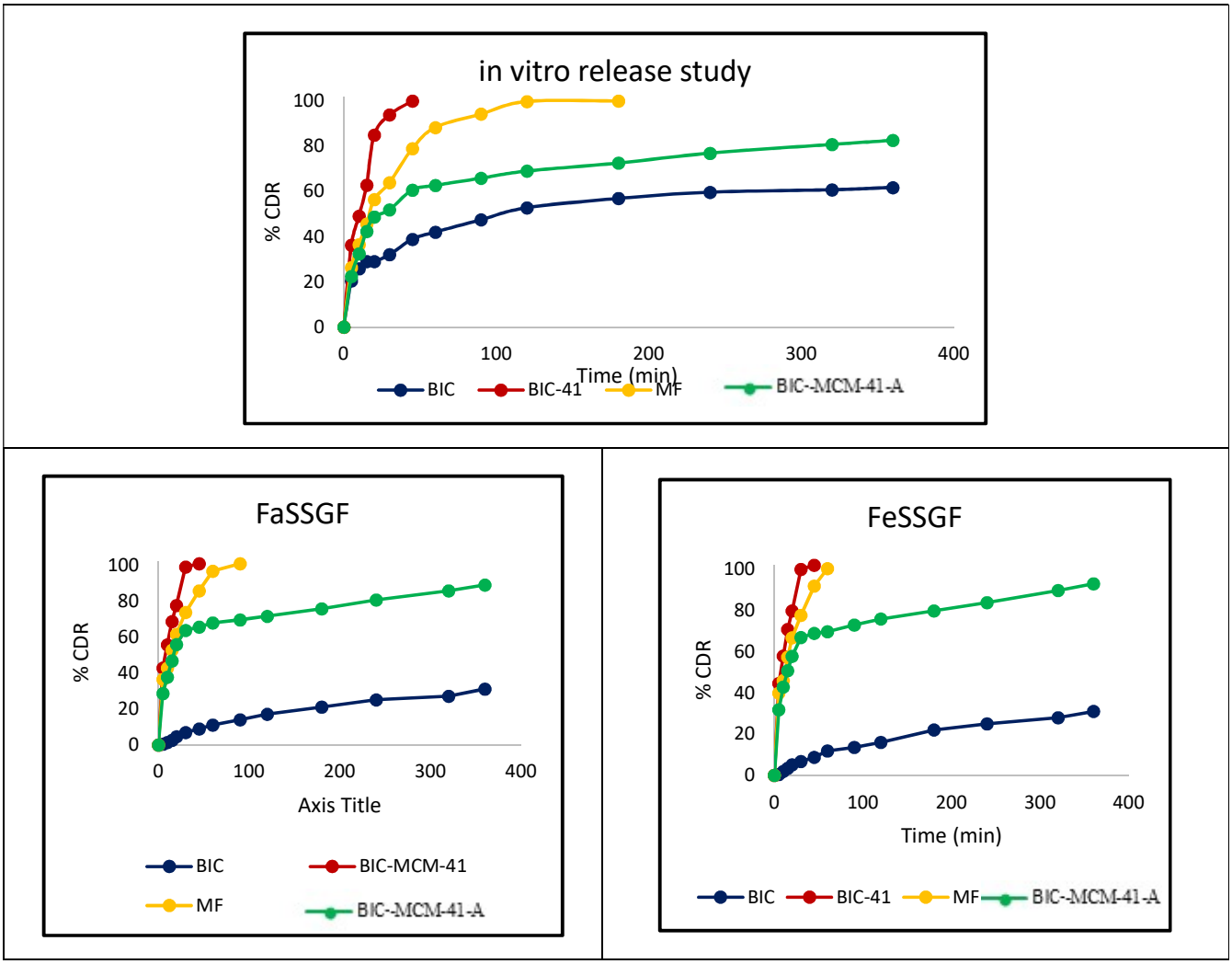

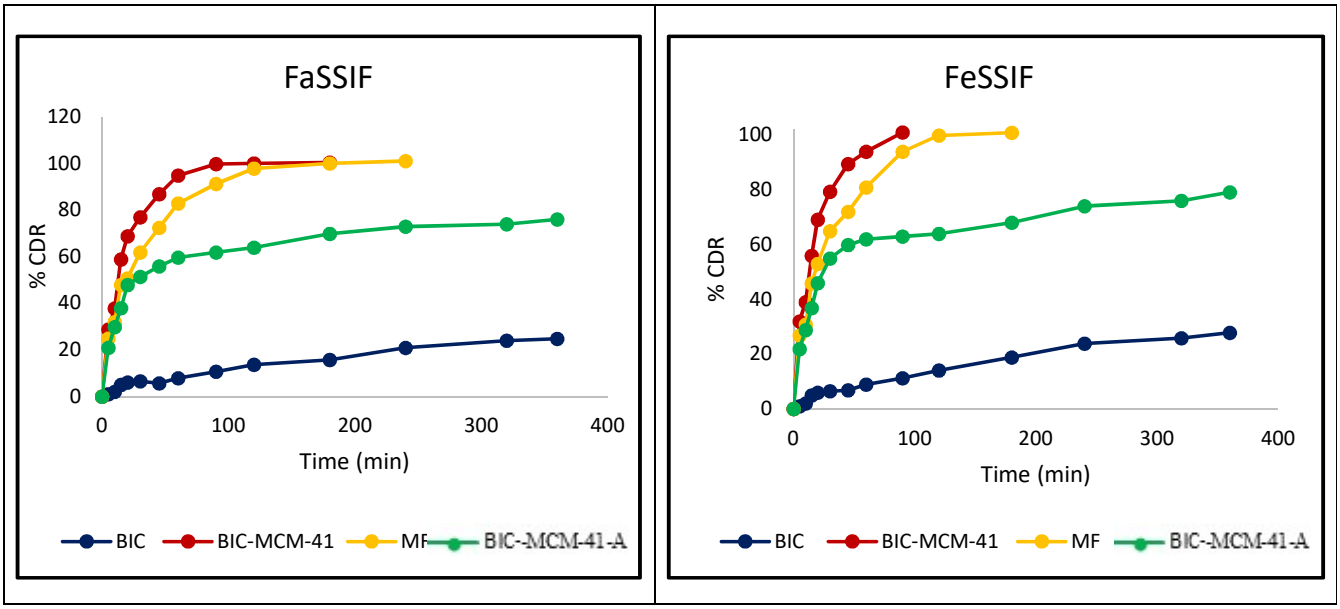

Figure 7.7. In vitro dissolution data for various formulations in different media.

Formulation	Statistical Parameters	Dissolution media	Dissolution model					
			Zero	First	Weibull	Higuchi	Hixon Crowell	Korsmeyer peppas
BIC-MCM-41	R^2	0.5%SLS in water	0.8898	0.9894	0.9900	0.9585	0.9840	0.9804
		0.5%SLS in FaSSGF	0.5206	0.9796	0.9848	0.9672	0.9720	0.9813
		0.5%SLS in FeSSGF	0.4807	0.9799	0.9862	0.9615	0.9707	0.9819
		0.5%SLS in FaSSIF	0.0139	0.9911	0.9936	0.8449	0.9403	0.9476
		0.5%SLS in FeSSIF	-0.0086	0.9907	0.9934	0.8426	0.9384	0.9521
BIC-MCM-41	AIC	0.5%SLS in water	69.43	41.25	38.00	48.89	41.55	44.88
		0.5%SLS in FaSSGF	59.21	37.11	37.07	40.44	39.33	40.52
		0.5%SLS in FeSSGF	59.88	37.13	36.46	41.67	39.75	40.39
		0.5%SLS in FaSSIF	94.22	47.17	47.82	75.72	66.18	66.88
		0.5%SLS in FeSSIF	94.45	47.59	48.17	75.88	66.50	65.99

BIC-MCM-41	**MSC**	0.5%SLS in water	-0.2918	3.19	3.63	2.27	3.23	2.77
		0.5%SLS in FaSSGF	-0.33	2.71	2.82	2.34	2.50	2.33
		0.5%SLS in FeSSGF	-0.45	2.79	2.89	2.14	2.42	2.32
		0.5%SLS in FaSSIF	-0.72	3.98	3.91	1.12	2.08	2.01
		0.5%SLS in FeSSIF	-0.75	3.92	3.86	1.09	2.03	2.08

Table 7.6. Statistical analysis of release profile of BIC-MCM-41

Formulation	**Statistical Parameters**	**Dissolution media**	**Dissolution model**					
			Zero	**First**	**Weibull**	**Higuchi**	**Hixon Crowell**	**Korsmeyer peppas**
BIC-MCM-41-A	**R^2**	0.5%SLS in water	-1.0709	0.4828	0.3995	0.9868	0.2041	0.9475
		0.5%SLS in FaSSGF	-1.3167	0.5656	0.2959	0.9853	0.1588	0.9585
		0.5%SLS in FeSSGF	-1.4610	0.6499	0.2376	0.9893	0.1417	0.9681
		0.5%SLS in FaSSIF	-1.003	0.3247	0.4367	0.9892	0.1023	0.9517
		0.5%SLS in FeSSIF	-0.9471	0.3854	0.4502	0.9786	0.1563	0.9427
BIC-MCM-41-A	**AIC**	0.5%SLS in water	136.90	117.47	119.56	70.14	123.51	87.46
		0.5%SLS in FaSSGF	139.19	115.76	122.52	72.37	125.01	84.88
		0.5%SLS in FeSSGF	140.77	113.47	124.37	68.62	126.02	81.93
		0.5%SLS in FaSSIF	134.62	119.40	116.86	65.47	123.39	85.64
		0.5%SLS in FeSSIF	135.03	118.89	117.33	75.88	123.32	87.67
BIC-MCM-41-A	**MSC**	0.5%SLS in water	-1.41	-0.026	-0.17	3.35	-0.45	2.11
		0.5%SLS in FaSSGF	-1.60	0.072	-0.41	3.17	-0.58	2.27
		0.5%SLS in FeSSGF	-1.70	0.24	-0.53	3.44	-0.65	2.49
		0.5%SLS in FaSSIF	-1.36	-0.27	-0.09	3.57	-0.55	2.22
		0.5%SLS in FeSSIF	-1.31	-0.16	-0.05	2.90	-0.48	2.06

Table 7.7. Statistical analysis of release profile of BIC-MCM-41-A

7.3.3.2 In vitro diffusion study

The pH responsive based release was investigated for BIC, BIC-MCM-41, BIC-MCM-41-A, BIC-FA-MSN and BIC-PAA-MSNs at PBS media of different pH *viz,* 5.6, 6.8 and 7.4 as a function of time (Fig 7.8). It was observed that BIC-PAA-MSNs exhibited a highly pH responsive behavior. Drug release from PAA-MSNs was found to varying inversely and decreased with increase in pH. Maximum BIC release at 72 h was observed at pH 5.6 with percentage cumulative release being 89.92±0.65%. The release at pH 6.8 and 7.4 was found to be 68.85±0.98 % and 30.72±0.72 % respectively. At lower pH PAA gets completely protonated leading to enhanced release of BIC due to weakened interactions. However, for BIC-MCM-41 NPs the release reached 98.72±0.82% at pH 5.6 within 48 h. Though, the release was up to 1.23 times faster in case of drug loaded bare silica when compared to BIC-PAA--MSN, no pH differentiating effect was seen, under stably due to absence of any pH responsive moiety on bare MCM-41. Further, PAA coating could also be held responsible for the slow release of BIC. A slight pH responsive behaviour was seen in case of BIC-MCM-41-A and BIC-FA-MSN but not as major as PAA-MSN. The release of BIC from PAA-MSN and MCM-41-A was faster than that of PAA-MSN.

However, at higher pH like 7.4 it might be possible that drug release could be hindered due to strong forces acting as a barrier. For determining the release mechanism involved the cumulative percentage release data were incorporated to three kinetic models for zero order, Higuchi and Korsmeyer Peppas model. The best fit model for determining release of BIC from MSNs matrix was found to be Korsmeyer Peppas model. PAA-MSNs exhibited n value lying across 0.43 and 0.85 which is a proof of existence of an anomalous diffusion mechanism. Anomalous diffusion combines both Fickian and Non-fickian diffusion. Both diffusion and swelling are relative. In case of anomalous transport polymeric relaxation and solvent diffusion both are almost similar in magnitudes. In case of n value up to 0.5 the BIC release is

mainly diffusion controlled. Here the rate of solvent diffusion is at a much higher level than the polymeric relaxation process. Furthermore, n value greater than 0.85 indicates swelling governed diffusion process. Swelling is credited to the expansion of polymer employed (9). An n value of greater than 1 means there exists a Super case II model. Here it was observed that for non-functionalized MCM-41 NPs the BIC release followed fickian diffusion and not much pH dependency was seen. However, in case of MCM-41-A, FA-MSNs and PAA-MSNs a highly pH responsive and sustained release was obtained for greater than 72 h. The anomalous transport mechanism was observed in these cases. Release mechanisms are summarized in Table 7.8.

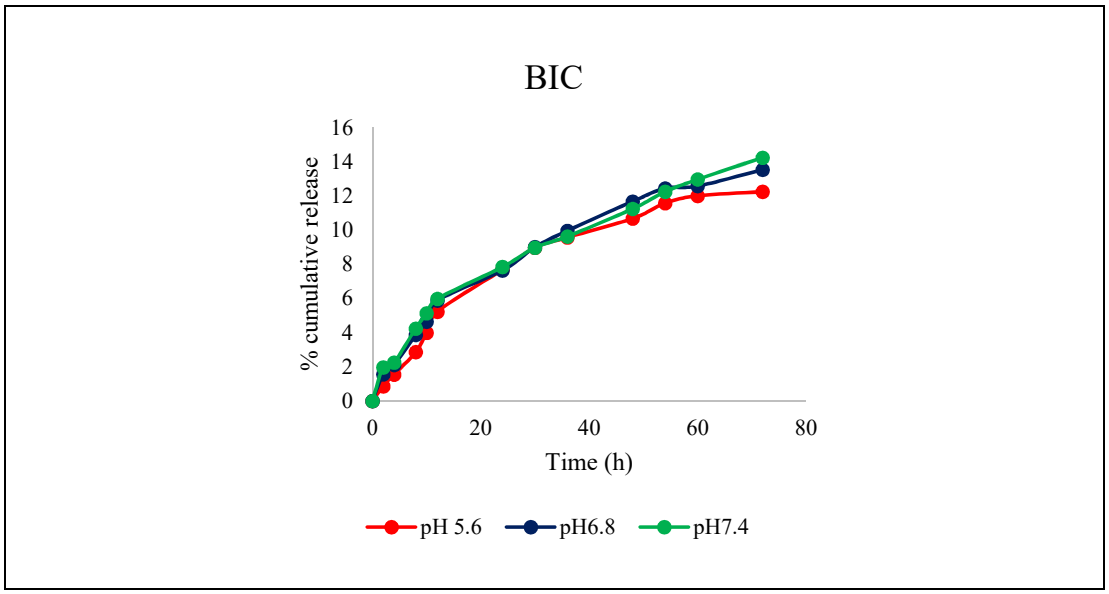

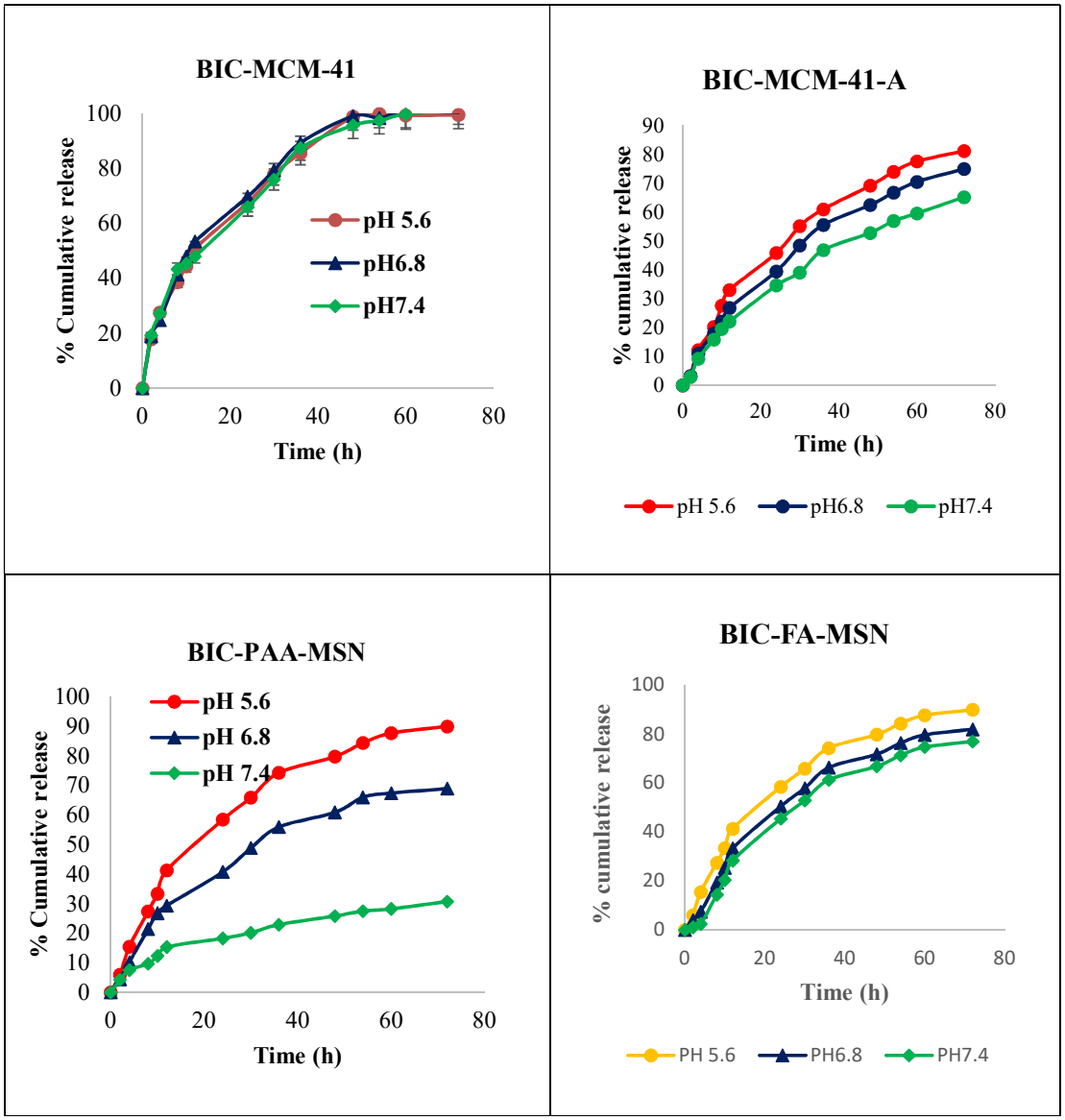

Figure 7.8. BIC release from various formulations at different pH.

Sr. No.	FORMULATION	pH	PARAMETERS	MODEL				
				Korsmeyer Peppas	Transport mechanism	Zero order	First order	Higuchi
1.	BIC-MCM-41	5.6	R^2	0.9871		0.6222	0.9829	0.9766
			AIC	72.68		113.79	75.59	77.61
			MSC	3.66		0.5071	3.44	3.29
			n	0.41	Fickian			
2.	BIC-MCM-41	6.8	R^2	0.9879		0.5818	0.9801	0.9696
			AIC	70.49		115.25	77.67	81.17
			MSC	3.87		0.3948	3.28	3.016
			n	0.40	Fickian			
3.	BIC-MCM-41	7.4	R^2	0.9880		0.6140	0.9779	0.9801
			AIC	70.03		113.62	76.45	75.10
			MSC	3.92		0.4736	3.33	3.43
			n	0.38	Fickian			
4.	BIC-MCM-41-PAA	5.6	R^2	0.9897		0.9448	0.9783	0.9768
			AIC	63.05		105.22	76.78	75.64
			MSC	3.42		1.102	3.28	3.377
			n	0.530	anomalous			
5.	BIC-MCM-41-PAA	6.8	R^2	0.9889		0.8068	0.9623	0.9774
			AIC	73.78		96.401	75.17	68.51
			MSC	3.58		1.265	2.89	3.41
			n	0.551	anomalous			
6.	BIC-MCM-41-PAA	7.4	R^2	0.9949		0.5608	0.6629	0.9667
			AIC	29.96		82.50	79.06	48.95
			MSC	4.242		0.3308	0.5952	2.9113
			n	0.479	anomalous			

Sr. No.	FORMULATION	pH	PARAMETERS	MODEL				
				Korsmeyer Peppas	transport mechanism	Zero order	First order	Higuchi
7.	BIC-MCM-41-A	5.6	R^2	0.9934		0.8564	0.9907	0.9745
			AIC	60.99		96.53	68.28	74.06
			MSC	4.31		1.58	3.75	3.30
			n	0.592	anomalous			
8.	BIC-MCM-41-A	6.8	R^2	0.9955		0.8921	0.9921	0.9700
			AIC	56.60		90.59	61.26	73.93
			MSC	4.49		1.87	4.13	3.16
			n	0.628	anomalous			
9.	BIC-MCM-41-A	7.4	R^2	0.9971		0.9007	0.9837	0.9719
			AIC	51.49		85.28	61.81	68.89
			MSC	4.56		1.96	3.76	3.22
			n	0.631	anomalous			
10.	BIC-FA-MSN	5.6	R^2	0.9942		0.7747	0.9897	0.9768
			AIC	57.66		105.22	76.78	75.64
			MSC	4.76		1.10	3.28	3.37
			n	0.53	anomalous			
11.	BIC-FA-MSN	6.8	R^2	0.9929		0.8534	0.9874	0.9880
			AIC	58.91		98.23	78.03	81.67
			MSC	4.59		1.57	3.12	2.89
			n	0.604	anomalous			
12.	BIC-FA-MSN	7.4	R^2	0.9943		0.9588	0.9840	0.9339
			AIC	65.16		93.55	80.69	87.19
			MSC	4.09		1.91	2.90	2.40
			n	0.668	anomalous			

Table 7.8. Statistical analysis of diffusion release profile of BIC-MSNs

7.3.4 In vitro cytotoxicity study

MTT assay of BIC-PAA-MSN and BIC-FA-MSN was performed on PC-3 and LNCaP cells (figure 7.9 and 7.10). Cell viability study for synthesized nanocarriers was performed on both the cell lines. Concentration range taken was (0.1-70 μg/mL) and for PC-3 and LNCaP cells respectively. The IC_{50} value was far low for BIC loaded PAA-MSN and FA-MSNs as compared to free BIC. The concentration range selected for study cytotoxicity assay was 0.1-

70 µg/mL. The IC_{50} value of BIC was found to be 16.24±0.37 and 25.72±0.84 µg/mL for LNCaP and PC-3 respectively. They were significantly reduced for BIC-PAA-MSNs as compared to BIC to 8.21±0.72 and 17.4±0.99 µg/mL for LNCaP and PC-3 cells respectively. Similarly, for BIC-FA-MSN the IC_{50} was found to be less than even 5 µg/mL at the end of 72 h. The percentage viability of cells decreased as the concentration of formulation increased.

The toxicity of synthesized nanoparticles was compared on Caco-2 cell lines (fig 7.11). Comparison of cytotoxicity was done amongst BIC, BIC-MCM-41 and BIC-MCM-41-A NPs. The MTT assay was performed providing an incubation time of 4 h. The results indicated relatively safer nature of MSNs on Caco-2 cells in the concentration range of 10-100 µg/mL. The percentage viability was found to be greater than 90 percent in all cases.

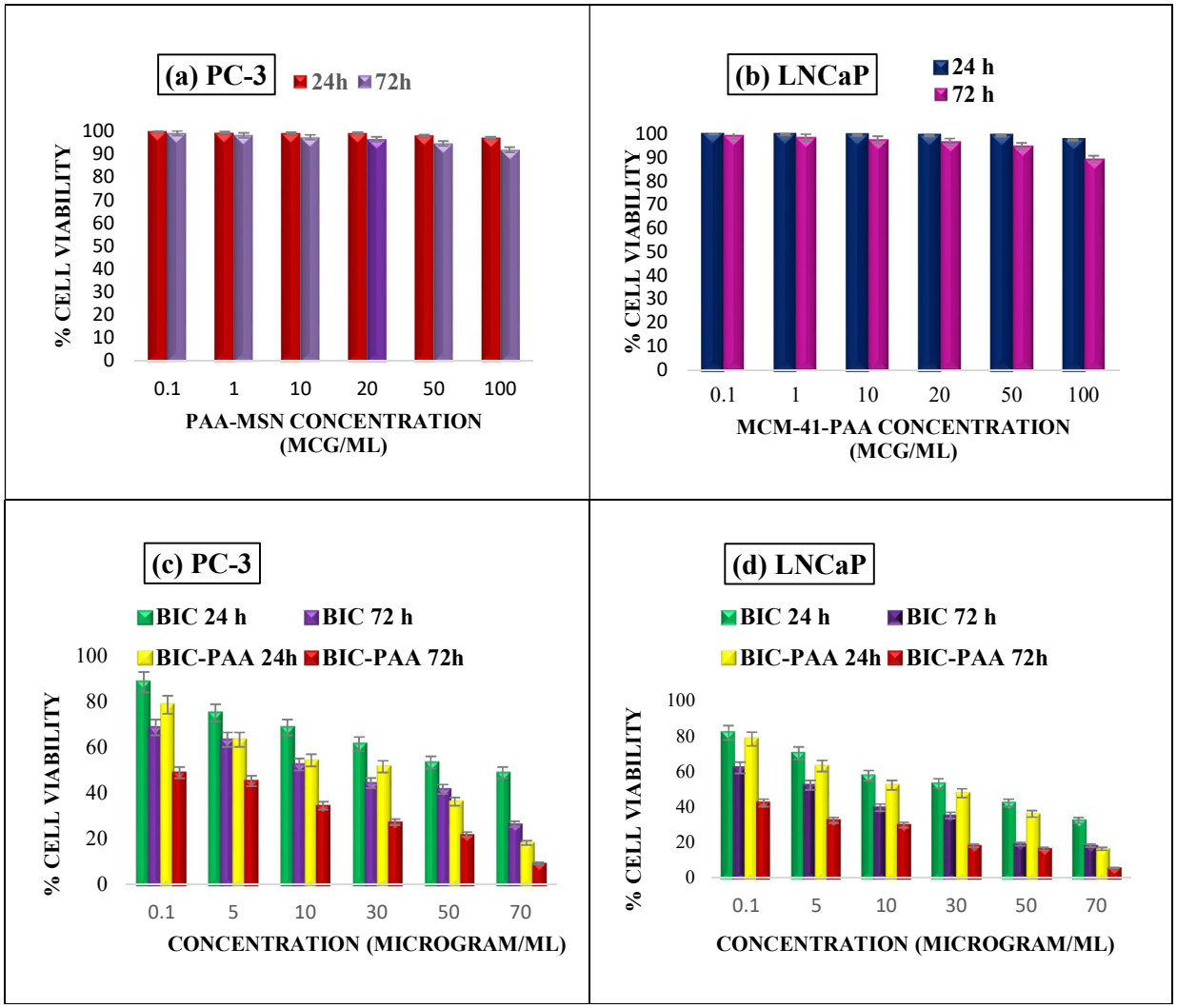

Figure 7.9. MTT Assay of BIC, BIC-PAA-MSNs on PC-3 and LNCaP cells.

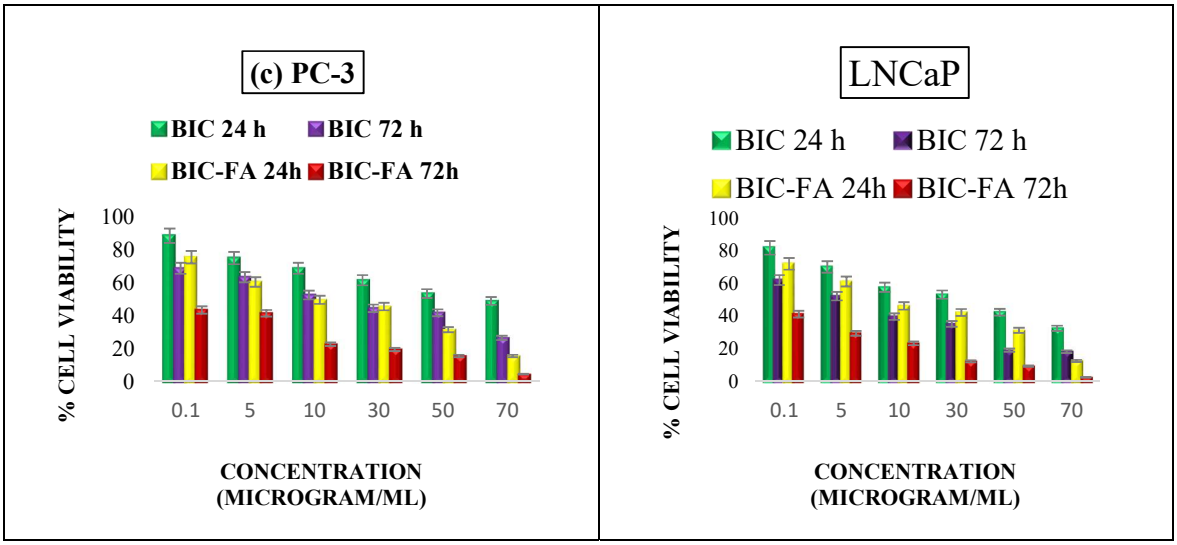

Figure 7.10. MTT Assay of BIC-FA MSNs

7.3.5 Caco-2 monolayer cell line permeability study:

From the results obtained in cell cytotoxicity assay concentration of 100 µg/mL was selected to be safe for proceeding further with cell permeability study. Experiment was conducted for BIC, BIC loaded MCM-41 and BIC-MCM-41-A from apical to basal compartment. Papp value was estimated for various formulations (Table 7.9). There was an improvement of 4.66-fold in permeability of with respect to BIC in case of BIC-MCM-41. Therefore, it could be concluded that BIC encapsulation into the mesoporous network proved to be beneficial in enhancing its permeability as well.

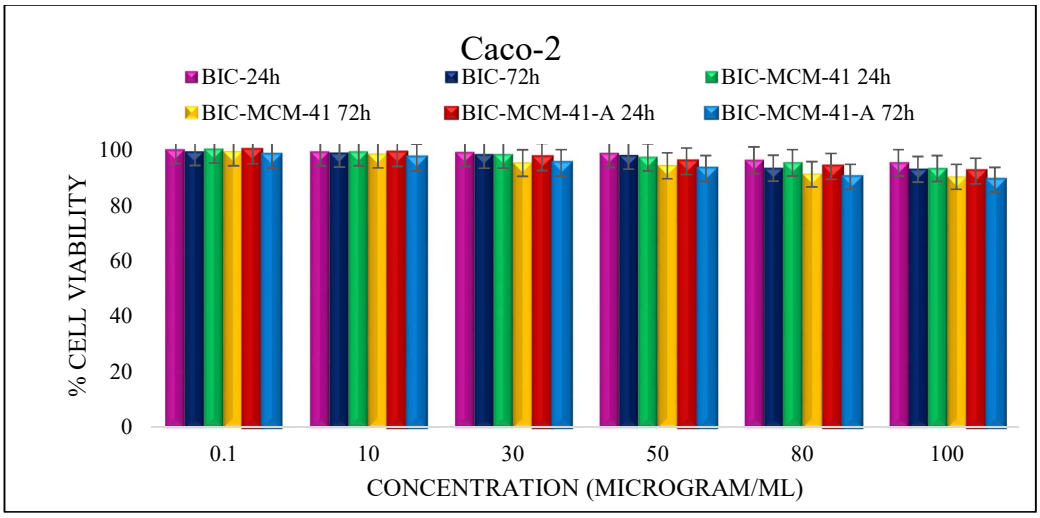

Figure 7.11. MTT assay on Caco-2 cells

Permeability (Papp) (cm/s)			
TIME (min)	**BIC**	**BIC 41**	**BIC-NH2-41**
30	0.65±0.04	4.96±0.72	3.56±0.51
60	1.52±0.22	15.67±1.26	9.93±1.38
90	3.81±0.56	25.49±1.89	13.32±1.66
120	5.93±0.87	32.88±2.04	19.57±2.17
180	6.99±1.07	38.15±2.98	25.24±2.56
240	9.82±1.39	43.07±3.01	30.08±2.82
300	11.12±1.84	49.83±3.47	31.82±3.05
Papp	**$1.96*10^{-2}$**	**$9.14*10^{-2}$**	**$5.31*10^{-2}$**

Table 7.9. Permeability determination of developed formulations

7.3.6 In vitro cellular uptake study

The results obtained for qualitative and quantitative cellular uptake study for MSN nanocarriers are discussed in section 6.3.6.

7.3.7 Evaluation of cell death mechanisms by apoptosis assay

The death mechanisms were adjudged by FACS protocol using Annexin V-FITC apoptosis detection kit. The cells were treated with BIC,BIC-MCM-41, BIC-MCM-41-A, BIC-PAA-MSN,BIC-FA-MSN NPs and free BIC for 24h. For LNCaP cells, total apoptosis was observed as 32.22%, 64.07%, 78.34% and 87.48% in cells treated with BIC-MCM-41, BIC-MCM-41-A, BIC-PAA-MSN and BIC-FA-MSN respectively. For PC-3 cells total apoptosis including early and late was 30.32%, 61.53%,82.24 % and 92.51% respectively for BIC-MCM-41, BIC-MCM-41-A, BIC-PAA-MSN and BIC-FA-MSNs. Free BIC could induce very less early apoptosis in the cells due to poor internalization into cells. Notably, drug loaded NPs led to early and late apoptosis induction in within 24 h in LNCaP cells. Remarkably FA-MSNs were capable of inducing both early and more late apoptosis at the same concentration (Figure 7.12). Also, they exhibited higher early and late apoptotic cells percentage than MCM-41-A NPs. It can be concluded that target group played a major role in giving this outcome. Almost similar results were obtained for PC-3 cells with more population found in late apoptotic stage than other MSNs or drug itself.

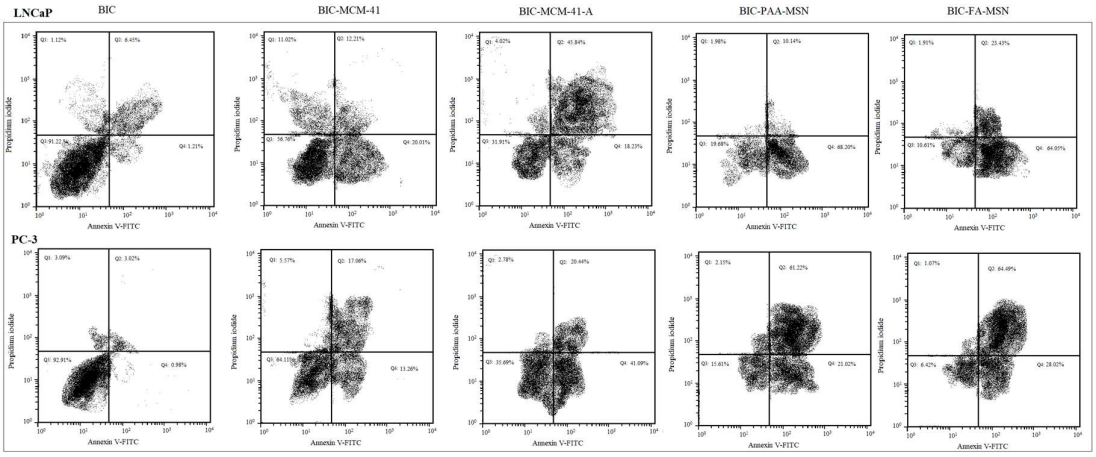

Figure 7.12. Apoptosis study of BIC and BIC loaded MSNs

7.3.8 Haemolysis study

Hem compatibility study was executed for synthesized NPs. Here TritonX100 treated RBCs

were taken as a positive control with significant lysis observed. Excellent hem compatibility was shown by all the synthesized NPs. The maximum haemolysis was observed in MCM-41-A with 2.1 % value, and 1.08 , 1.25 and 0.96 %, 0.85% for BIC-MCM-41, BIC-MCM-41-A, BIC-FA-MSN and BIC-PAA-MSNs respectively. All the results obtained were meeting the safety criteria of <5%. The microscopic images are shown in figure 7.13. Thus, haemolysis study established biosafety of the synthesized NPs (10, 11).

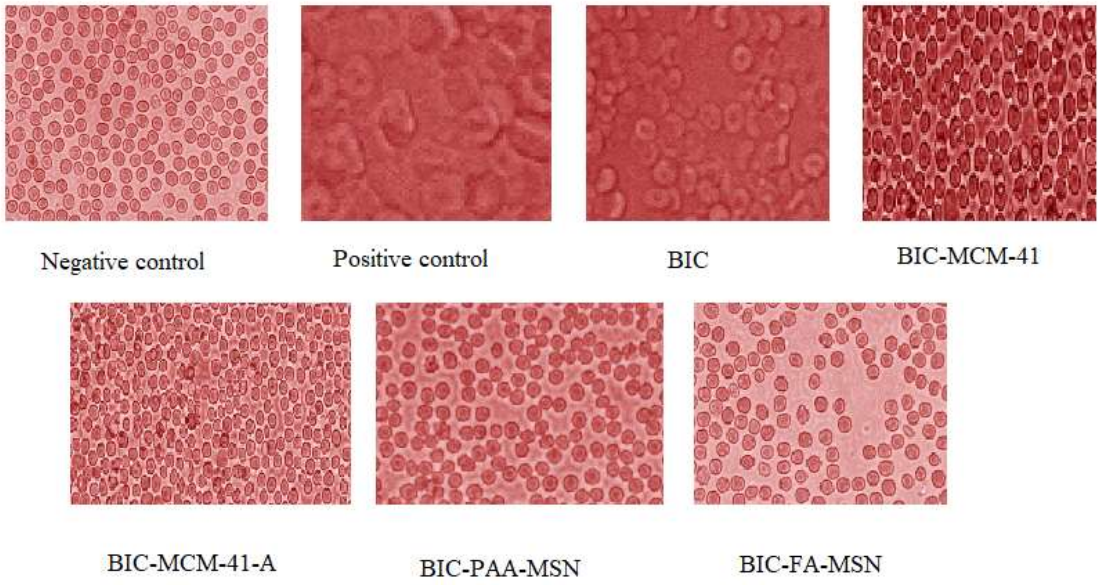

Figure 7.13. Microscopic images of the formulations tested for haemolysis

7.3.9 In vivo pharmacokinetic study

7.3.9.1 Pharmacokinetic study for oral formulation

Poor bioavailability of BIC is attributed to its limited solubility. To determine the oral bioavailability of BIC pharmacokinetic study of BIC, BIC-MCM-41 and BIC-MCM-41-A was carried out in male swiss albino mice (figure 7.14). All the blood samples collected were adequately processed and analysed by a well-developed and validated RP-HPLC-FL method. Different pharmacokinetic parameters like $t_{1/2}$, AUC etc were calculated for administered samples and the results are summarized in Table 7.10. The outcome gave a significant

increment in drug plasma concentration ($p<0.05$) on administration of formulated nanoparticle as compared to drug alone. Cmax was highest for BIC-MCM-41 NPs. Highest bioavailability and AUC were obtained using MCM-41 carriers. The BA of BIC-MCM-41 MSNs was 2.61 and 1.38 times more as compared to BIC and MF respectively. Whereas, in case of functionalized matrix the BA was enhanced 1.71 times the drug solution.

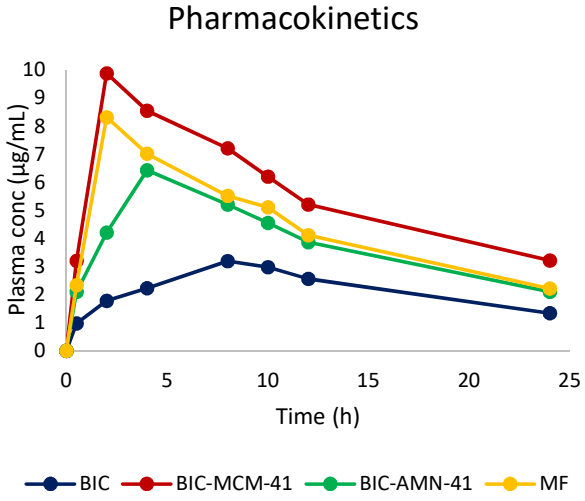

Figure 7.14. Oral Pharmacokinetic study of BIC and BIC loaded MSNs along with MF.

PARAMETERS / SAMPLE	$T_{1/2}$	T_{max}	C_{max}	AUC $_{0\text{-inf\_obs}}$	MRT $_{0\text{-inf\_obs}}$
BICALUTAMIDE	12.55	8	3.24	76.58	20.89
BIC-41	13.61	2	9.88	199.23	20.55
BIC-MCM-41-A	12.38	4	6.43	130.99	19.21
MARKETED FORMULATION	11.66	2	8.32	144.26	17.61

Table 7.10. Oral pharmacokinetic study of MSNs

7.3.9.2 Pharmacokinetic study for parenteral formulation

The pharmacokinetic parameters of all the 5 different samples administered were quite different from each other). Free BIC exhibited a more rapid clearance from blood with $t_{1/2}$ 9.2 h and

AUC 89.09 µg/mL h. BIC loaded MCM-41 NPs also exhibited a half-life of 12.25 h, Whereas, BIC-PAA-MSN exhibited a slow and steady clearance with longer $t_{1/2}$ 29.61 h and higher AUC 423.14 µg/mL h (3.21 and 4.74 times) as compared to free BIC. Higher $t_{1/2}$ indicates the ability of nanocarriers to accumulate at tumour site and give enhanced therapeutic effect (Table 7.11). BIC loaded nanocarriers had a slower plasma elimination rate and longer circulation time than BIC alone. BIC-FA-MSN also exhibited a half-life of 16.22 h and AUC of 186.19 µg/mL h. BIC-MCM-41-A showed t1/2 and AUC of 11.93 min 178.81 µg/mL h respectively (figure7.14).

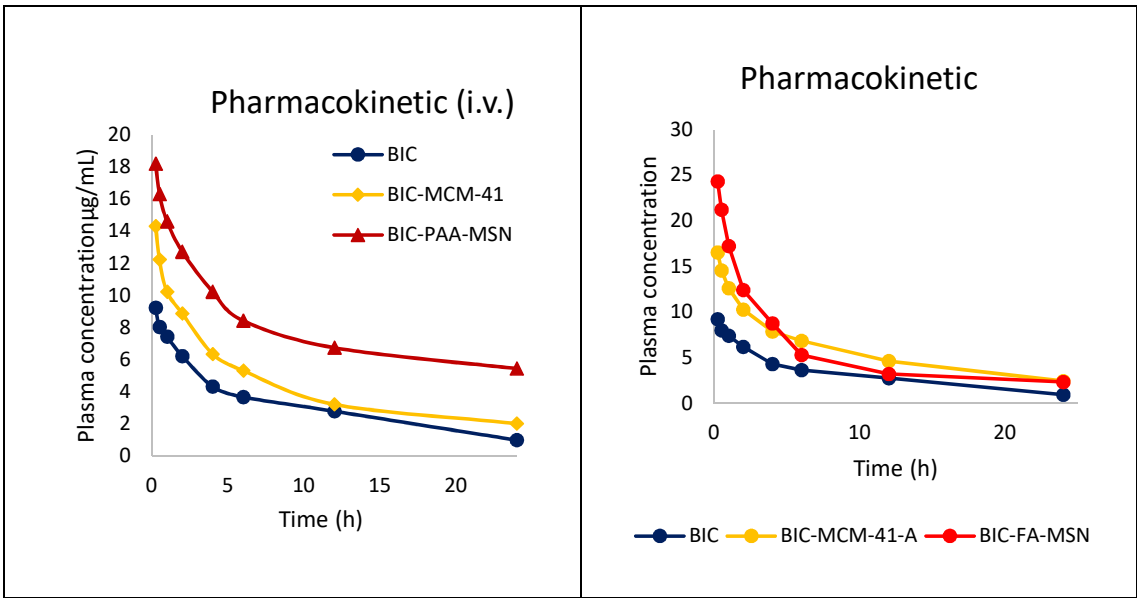

Figure 7.14. Intravenous pharmacokinetic study of BIC and BIC loaded MSNs

Group	$t_{1/2}$ (h)	AUC $_{0-t}$ (µg/ml*h)	Cl (mg)/(µg/ml)/h	V_{ss} (mg)/(µg/ml)	MRT (h)	C_{max} (µg/ml)
BIC	9.42	89.09	0.1122	1.37	12.25	9.23
BIC-41	12.25	141.69	0.0705	1.16	16.46	14.32
BIC-MCM-41-A	11.93	178.81	0.0559	0.896	16.02	16.54
BIC-PAA-41	29.61	423.14	0.0236	0.96	41.01	18.21
BIC-FA-MSN	16.22	186.19	0.0537	1.023	19.059	24.33

Table 7.11. Pharmacokinetic data of i.v. administered MSNs.

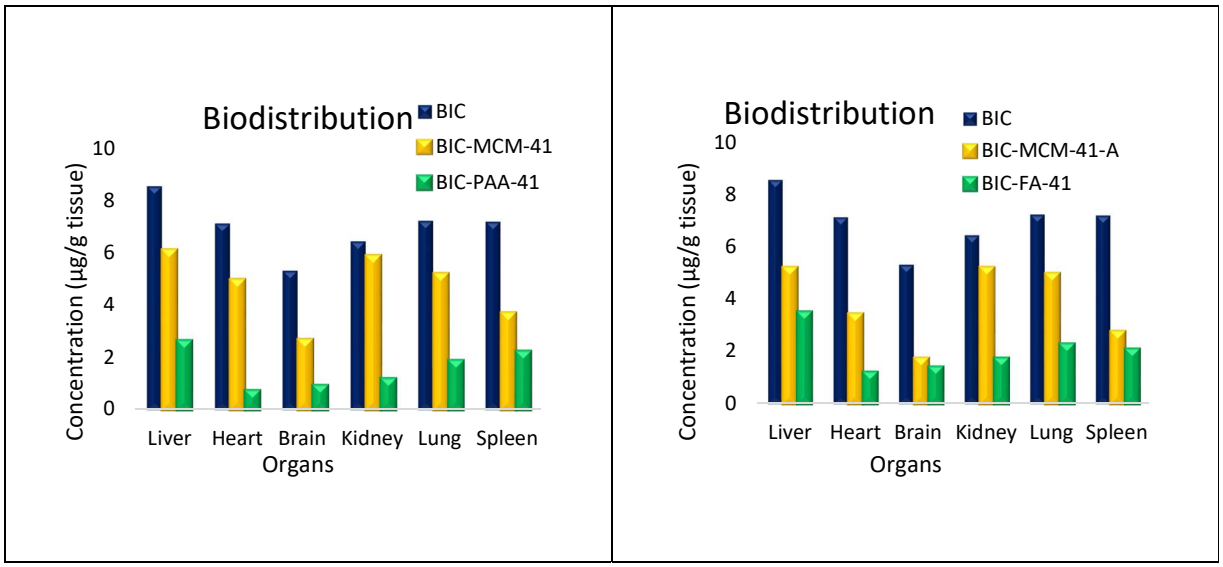

Figure 7.15. Biodistribution study of BIC and BIC loaded MSN formulations

The biodistribution study data revealed that accumulation or toxicity in major organs was less in case of drug loaded MSNs as compared to BIC alone (figure 7.15). The histological examination of various major organs post-formulation administration revealed no significant lethality. Fig 7.16. shows H&E sections of various organs of healthy swiss albino mice 24 h after intravenous administration. Compared with the control group there were no major differences or inflammation observed in case of mice treated with BIC-PAA-MSNs and BIC-FA-MSNs after 24h duration as well.

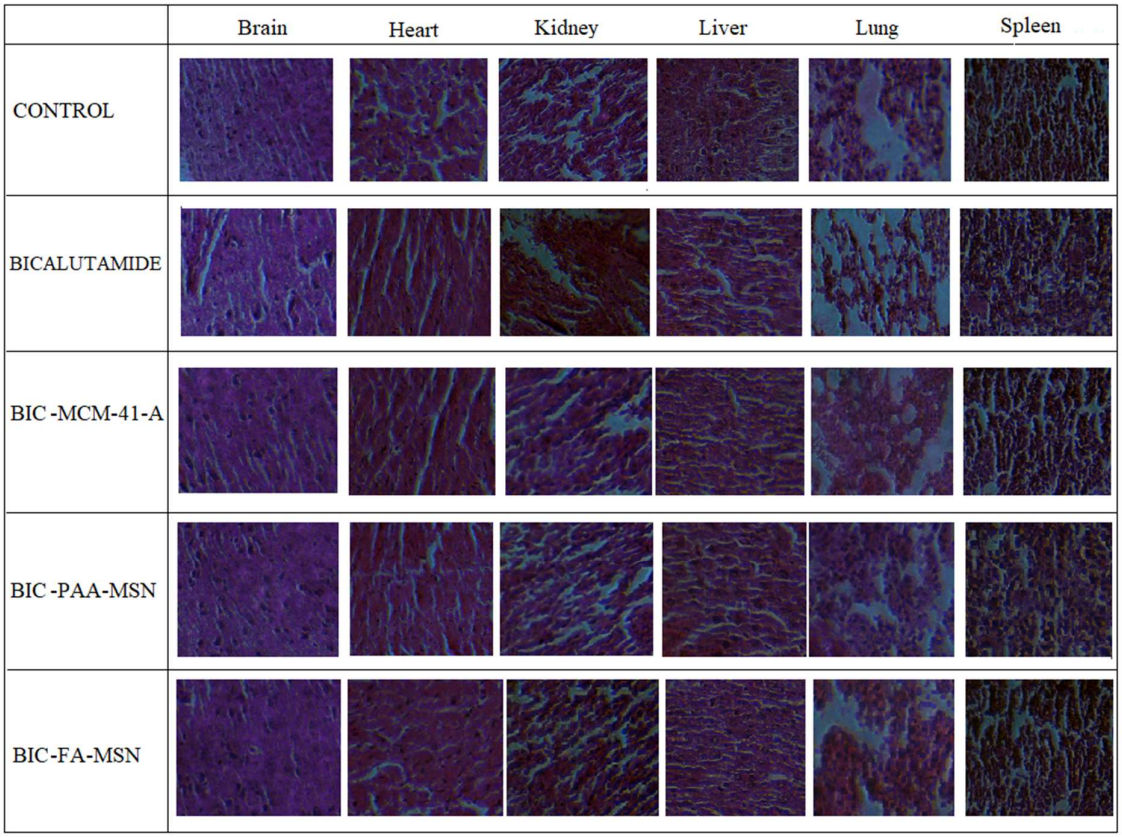

Figure 7.16. Histological examination of major tissue post administration of BIC and BIC loaded MSNs.

7.3.10 Stability study of mesoporous silica nanoparticles

The DSC (Figure 7.17 and 7.18) and SXRD data revealed that the synthesized MSNs were stable at 40±2 ºC and 75±5 %RH for the tested duration. There is no degradation observed in the drug loaded MSNs spectra suggesting absence of any drug leakage. Further, identical LXRD pattern at 0^{th} month and after 6^{th} month (Figure 7.18) revealed the intactness of mesoporous skeleton and stability.

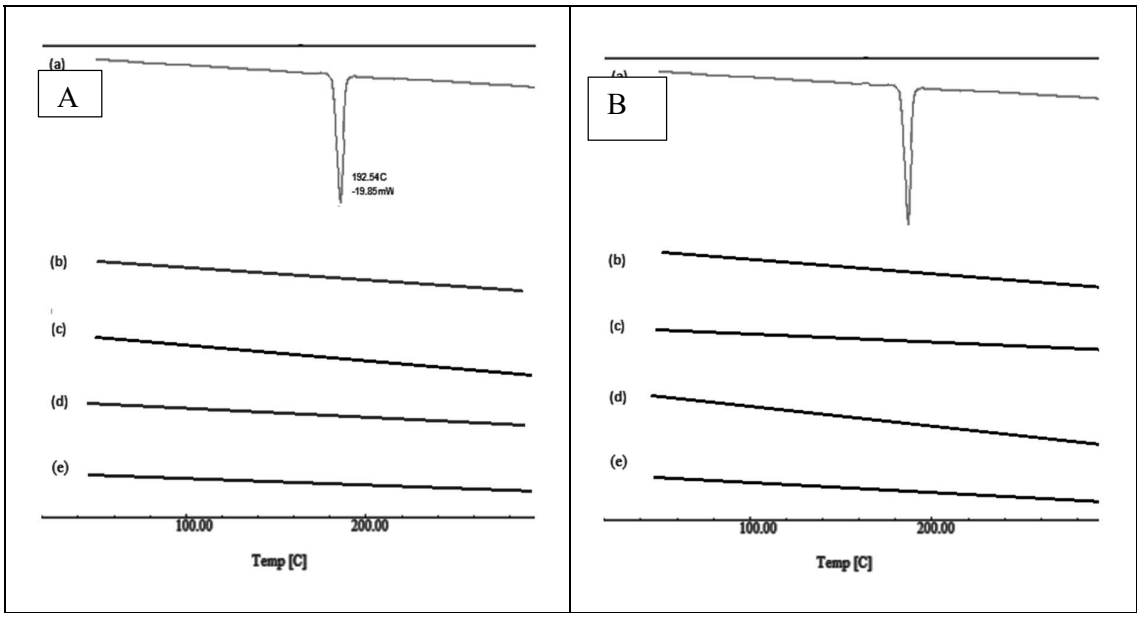

Figure 7.17. DSC thermogram of (a) BIC (b)BIC-MCM-41 (c) BIC-MCM-41-A (d) BIC-PAA-MSN (e) BIC-FA-MSN at 0^{th} (A)and 6^{th} (B) month

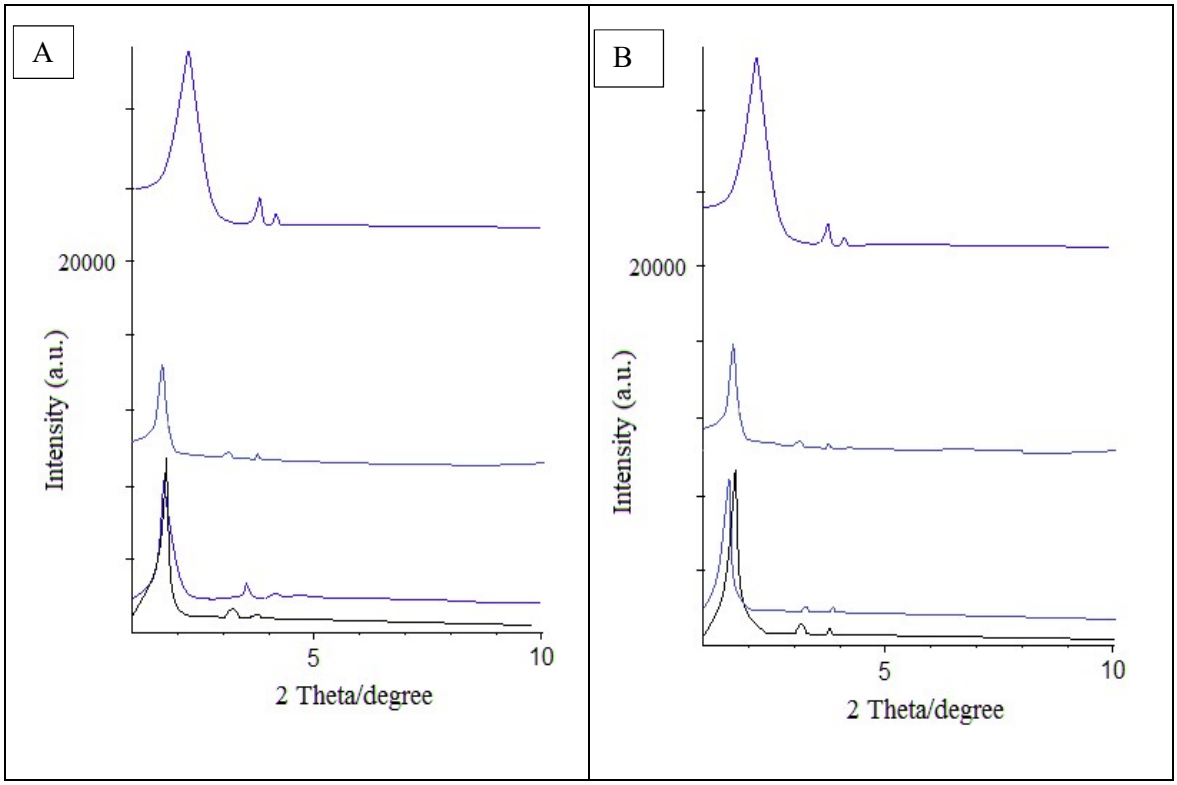

Figure 7.18. LXRD data for (a) BIC-MCM-41, (b) BIC-MCM-41-A (c) BIC-PAA-MSN and (d) BIC-FA-MSN at 0^{th}(A) and 6^{th} month (B).

7.4 Conclusion

The results obtained were suggestive of successful BIC encapsulation into the MSN skeleton both bare and surface functionalised. A significant enhancement in its dissolution rate and bioavailability with 3.12 and 2.61 times respectively as compared to BIC was obtained for BIC-MCM-41. Whereas the results obtained were 1.86 and 1.38 respectively for BIC-MCM-41-A. This could aid in dose reduction and enhanced efficacy at the same time overcoming the solubility limitations. The increment in dissolution and bioavailability could also lead to dose reduction. The permeability of BIC-MCM-41 NPs and BIC-MCM-41-A NPs were enhanced 4.66 and 2.71 times respectively with respect to BIC. The apoptotic assay revealed that BIC-PAA-MSN and BIC-FA-MSN were able to induce a higher percentage of apoptosis(LNCaP 78.34% and 87.48% and PC-3 82.24 % and 92.51% for BIC-PAA-MSN and BIC-FA-MSN respectively) than necrosis and hence caused a programmed cell death. Further biosafety of the nano formulation was established by results obtained from haemolysis, biodistribution study and histological examination. All the formulation exhibited lysis within the acceptable range of less than 5% and histological images were similar to the ones obtained for control ruling out any possible harm to healthy organs due to formulation. Thus, mesoporous silica nanoparticles could serve as an ideal candidates to provide an effective and targeted treatment for cancer patients. This could lead to a sure shot treatment and increased life expectancy with highly diminished side effects.

7.5 References:

1. Cockshott ID. Bicalutamide. Clinical pharmacokinetics. 2004;43(13):855-78.

2. Kolvenbag G. The prostate cancer continuum: the role of bicalutamide (Casodex®). The Prostate Journal. 2001;3(1):2-13.

3. Parihar JS, Kim IY. Second-Line Hormonal for Castrate-Resistant Prostate Cancer. Prostate Cancer: Elsevier; 2016. p. 533-40.

4. Kim TH, Kim M, Park HS, Shin US, Gong MS, Kim HW. Size-dependent cellular toxicity of silver nanoparticles. Journal of biomedical materials research Part A. 2012;100(4):1033-43.

5. Sun J-T, Hong C-Y, Pan C-Y. Fabrication of PDEAEMA-coated mesoporous silica nanoparticles and pH-responsive controlled release. The Journal of Physical Chemistry C. 2010;114(29):12481-6.

6. Kachbouri S, Mnasri N, Elaloui E, Moussaoui Y. Tuning particle morphology of mesoporous silica nanoparticles for adsorption of dyes from aqueous solution. Journal of Saudi Chemical Society. 2018;22(4):405-15.

7. Shah PV, Rajput SJ. A comparative in vitro release study of raloxifene encapsulated ordered MCM-41 and MCM-48 nanoparticles: a dissolution kinetics study in simulated and biorelevant media. Journal of Drug Delivery Science and Technology. 2017;41:31-44.

8. Shah P, Rajput SJ. Amine decorated 2d hexagonal and 3d cubic mesoporous silica nanoparticles: A comprehensive dissolution kinetic study in simulated and biorelevant media. Journal of Dispersion Science and Technology. 2018:1-19.

9. Jin S, Liu M, Chen S, Gao C. A drug-loaded gel based on polyelectrolyte complexes of poly (acrylic acid) with poly (vinylpyrrolidone) and chitosan. Materials Chemistry and Physics. 2010;123(2-3):463-70.

10. Daryasari MP, Akhgar MR, Mamashli F, Bigdeli B, Khoobi M. Chitosan-folate coated mesoporous silica nanoparticles as a smart and pH-sensitive system for curcumin delivery. Rsc Advances. 2016;6(107):105578-88.

11. Li J, Zheng L, Cai H, Sun W, Shen M, Zhang G, et al. Polyethyleneimine-mediated synthesis of folic acid-targeted iron oxide nanoparticles for in vivo tumor MR imaging. Biomaterials. 2013;34(33):8382-92.